Fluid inclusions as a monitor of progressive grain-scale deformation during cooling of the Papoose Flat pluton, eastern California

Nancy A. Brauer

Thesis submitted to the Faculty of the
Virginia Polytechnic Institute and State University
in partial fulfillment of the requirements for the degree of

Master of Science
in
Geological Sciences

APPROVED: _____
R. J. Bodnar, Co-Chair

_____
R. D. Law, Co-Chair

_____
R. J. Tracy

March 27, 1998
Blacksburg, Virginia

Keywords: Fluid Inclusions, Deformation,
Brittle-Ductile Transition, Papoose Flat pluton

Fluid inclusions as a monitor of progressive grain-scale deformation during cooling of the Papoose Flat pluton, eastern California

Nancy A. Brauer

(ABSTRACT)

Analyses of fluid inclusions and microstructures within the Papoose Flat pluton were used to investigate the chemistry and temperatures of fluids circulating with the pluton during cooling. Based on previous microstructural analyses, the interior of this late Cretaceous granitic to granodioritic pluton has been divided into three domains: i) a central core characterized by magmatic microstructures, ii) a middle domain of high temperature (>500°C) solid-state deformation, and iii) an outermost domain characterized by relatively low temperature (<500°C) solid-state deformation. According to previously published anisotropy of magnetic susceptibility analyses and pluton cooling models, plastic flow occurred in both the outer part of the pluton and within its aureole rocks while the core of the pluton was still molten. Solid-state deformation is proposed to have stopped when the pluton interior cooled through its solidus less than 100,000 years after magma emplacement.

Microstructural analysis of samples from all three domains confirmed the transition from magmatic flow in the core of the pluton to solid-state deformation at the pluton margin. However, weakly developed solid-state microstructures overprint the dominant magmatic microstructures in samples from the core domain. The existence of solid-state microstructures in all three domains indicates that deformation continued during and after crystallization of the interior of the pluton.

Two phase, low salinity (< 26 wt% NaCl equivalent), liquid-rich aqueous fluid inclusions predominate within both quartz and feldspar grains in all samples. Throughout the pluton, the majority of fluid inclusions are hosted by deformed grains. Feldspar-hosted primary inclusions are associated with sericitic alteration. Inclusions were also observed in feldspar as secondary or pseudosecondary inclusions along fractures. Inclusions in quartz are frequently found near lobate grain boundaries or near triple junctions; linear pseudosecondary inclusion assemblages are commonly truncated against lobate boundaries between adjacent quartz grains, indicating that discrete microcracking events occurred during plastic deformation.

Homogenization temperatures overlap for all three microstructural domains. Coexisting andalusite and cordierite in the contact aureole, and the intersection of the Mus + Qtz

dehydration reaction with the granite solidus, indicate trapping pressures between 3.8 and 4.2 kb. Ninety-eight percent of the calculated fluid inclusion trapping temperatures at 3.8 - 4.2 kb are below the granite solidus of 650°C. Seventy-six percent of the trapping temperature data fall within the more restricted range of 350-500°C; i.e. at temperatures which are lower than the commonly cited brittle-ductile transition temperatures for feldspar at natural strain rates, but above those for quartz. No correlation could be established between trapping temperatures and either host mineral or microstructural domain within the pluton.

The similar, relatively low trapping temperatures indicate that the majority of inclusions preserved in all three domains were trapped during the late low strain magnitude stages of solid-state deformation. The most common fluid inclusion trapping temperatures (400-500°C) in all three microstructural domains are similar to the deformation temperatures indicated by microstructures and crystal fabrics in the outer part of the pluton; these trapping temperatures are obviously lower than temperatures associated with contemporaneous solid state and magmatic flow in the pluton interior. The similar trapping temperatures within the pluton core and margin must indicate that the inclusion-trapping event migrated from the margin to the core of the pluton as it cooled, because fluid inclusions would rapidly equilibrate to a density appropriate for the PT conditions of their host minerals.

ACKNOWLEDGMENTS

Field and laboratory work was funded by grants from the Geological Society of America (#5780-96), Sigma Xi (#8033), and the Virginia Tech Graduate Student Assembly to N. A. Brauer, National Science Foundation grants EAR-9506525 to R. D. Law; and EAR-9526668 to R. J. Bodnar.

This Master's thesis could not have been accomplished without the funding, guidance, and help of Bob Bodnar and Rick Law, the co-advisors of this study. I am grateful to them and Bob Tracy for their interest, advice, and willingness to serve as committee members. Many thanks go to Michel de Saint Blanquat for discussion in the field and for providing several additional samples. The support and contributions of Paige Baldassaro, Theresa Denson, Ginger Vaughn, Amy Johnson, Kelly Rose, Sven Morgan, Jing Leng, Anurag Sharma, Frank Harrison, Csaba Szabo, and Jim Student are greatly appreciated. I would especially like to thank the friendly and helpful staff and graduate students at the Department of Geological Sciences. Last but not least, many thanks go to my family and Marc DeBonis for all of their moral support.

TABLE OF CONTENTS

LIST OF FIGURES

INTRODUCTION

In recent years experimental rock deformation studies (e.g. Arzi 1978; Van Der Molen & Paterson 1979; Tullis &Yund 1987, 1992) have successfully reproduced a range of microstructures which appear similar to those observed in naturally deformed granites. These experimental studies have demonstrated that the type of microstructures which progressively develop during deformation is strongly controlled by both intrinsic and extrinsic variables such as mineralogy, temperature, strain rate, etc. Given that particular experimentally produced microstructures tend to form under specific ranges of temperature and strain rate conditions, it is tempting to use similar microstructures found in naturally deformed granites as qualitative indicators of deformation conditions (Gapais & Barbarin 1986, Blumenfeld & Bouchez 1988, Gapais 1989, Paterson et al. 1989, Bouchez et al. 1992, Hirth & Tullis 1992, Miller and Patterson 1994, Kruhl 1996). However, experimental microstructures are produced at strain rates up to eight orders of magnitude faster than generally accepted natural strain rates of $10^{-13}$to $10^{-14}s^{-1}$ (e.g. Price 1975, Pfifner & Ramsey 1982, Paterson & Tobisch 1992).

This study of the Papoose Flat pluton was initially undertaken to assess the validity of using experimental microstructures as deformational geothermometers. The variety of deformational microstructures created at geological strain rates in the Papoose Flat pluton makes this location a natural laboratory. Temperatures of fluid inclusions from host grains displaying different microstructures were expected to record temperatures of deformation which would be compared with the results of the experimental studies. However, the trapping temperatures obtained in this study indicate that, at least in the case of the Papoose Flat pluton, fluid inclusions do not provide a record of early magmatic deformational conditions. The majority of fluid inclusion trapping temperatures are higher than the generally accepted temperatures associated with the quartz brittle-ductile transition and lower than the feldspar brittle-ductile transition temperatures. This suggests that many of the inclusions preserved in quartz grains, particularly those aligned in linear arrays, may be associated with localized high strain rate pulses which would have temporarily raised the brittle-ductile transition temperature. Although the fluid inclusions indicate temperatures consistent with crystal plasticity and recrystallization for quartz, the data only represent the last low strain magnitude stages of solid-state deformation at temperatures below the brittle-ductile transition for feldspar and above the upper limit of the quartz brittle-ductile transition.

GEOLOGICAL SETTING

The Papoose Flat pluton is located in the Inyo Mountains of eastern California (Fig. 1). The 83 Ma U/Pb monazite age (Miller 1996) makes the granitic to granodioritic pluton one of the

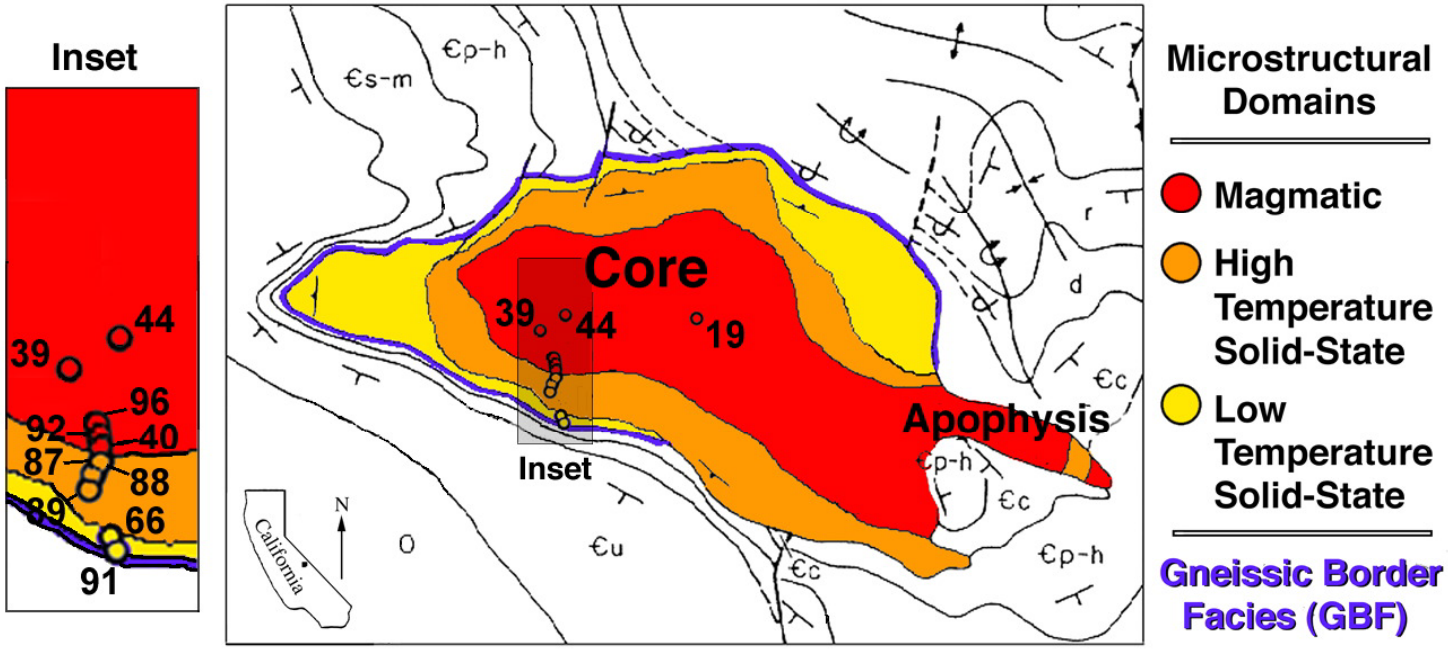

Figure 1. Map of sample localities (open circles) and the location of microstructural and mesoscopic fabric domains within the Papoose Flat pluton. Microstructural domains after St. Blanquat et al. (1994); position of gneissic border facies around the western and southern margins of the pluton after Sylvester et al. (1978), position of border facies on the northwestern margin of the pluton after St. Blanquat et al. (1994).

youngest of several Mesozoic plutons in the Inyo mountains considered to be satellites of the Sierra Nevada batholith located 15 to 20 km to the west across Owens Valley (Bateman et al. 1963, Bateman 1992). The pluton was emplaced into Precambrian and Paleozoic metasedimentary rocks (albite-epidote facies or lower - Ernst 1996) located in the SW dipping limb of the Inyo Anticline, and is concordant with the Cambrian age Poleta and Harkless formations along its western border, but is locally discordant along its eastern margin (Nelson et al. 1972, Sylvester et al. 1978). Comparison with regional stratigraphic thicknesses indicates that strata between the Cambrian Campito Formation and the late Cambrian Bonanza King Formation (the Poleta, Harkless, Saline Valley, Mule Spring, and Monola formations, Sylvester et al. 1978) in the western part of the aureole of the pluton have been structurally thinned by up to 90% during pluton emplacement (Nelson et al. 1972, Sylvester et al. 1978).

The K-feldspar megacrysts that occur throughout the pluton and in satellite dikes within the aureole at the eastern end of the pluton complicate its petrologic classification. Ross (1965) first classified the average composition as a porphyritic quartz monzonite. Neglecting the megacrysts moves the composition into the granodiorite field (Ross 1965). Later geochemical analyses by Brigham (1984) indicate a compositional variation spanning the granite and granodiorite fields as defined by LeMaitre (1989) and Streckeisen (1976). For simplicity, this paper will refer to the Papoose Flat pluton as a granite.

Emplacement pressures of the Papoose Flat pluton are well constrained by mineral assemblages and metamorphic reactions in the pluton and aureole rocks. Sylvester et al. (1978) proposed emplacement of the pluton at 9.2 km depth assuming a 35° limb dip, corresponding to a lithostatic pressure of 2.2 kb. Nyman et al. (1995) increased the calculated emplacement pressure range to 3 - 4 kb based on the coexistence of cordierite (Crd) and andalusite (And) in the contact aureole. Ernst (1996) cites a similar pressure range of 3±1 kb due to the absence of Ky and St in aureole rocks surrounding Jurassic-age plutons in the White-Inyo mountains. The emplacement pressure is further constrained to a minimum of 3.8 kb by the intersection of the muscovite (Mus) + quartz (Qtz) dehydration reaction and the granite solidus (Kerrick 1972) and a maximum of 4.2 ± 0.3 kb from the aluminosilicate triple point of Bohlen et al. (1991).

The pluton has been subdivided into separate domains using both macroscopic grain shape fabrics (Sylvester et al. 1978) and microstructural grain scale features (St. Blanquat et al. 1994). Three macroscopic fabric domains are evident in the pluton itself, a gneissic border facies, core zone, and an apophysis located at the eastern end of the pluton (Fig. 1). The gneissic border facies is located along the northwestern, western, southern (Sylvester et al. 1978), and northeastern (St. Blanquat et al. 1994) margins of the pluton. It is characterized by a strongly developed foliation oriented parallel to the pluton margin and surrounding foliation in the highly attenuated aureole rocks. A N-NW trending, gently plunging stretching lineation lies in the plane of foliation and is oriented subperpendicular to the long axis of the pluton. Lineation and

foliation are most strongly developed in the western half of the pluton and aureole rocks. Penetrative deformation is present throughout the western half of the aureole, while the eastern half (particularly around the apophysis) is characterized by hornfels textures. The central core zone of the pluton is composed of porphyritic granite generally lacking any obvious macroscopic grain shape fabric. The occurrence of elongate K-feldspar megacrysts, accounting for approximately 10% of the rock, was used by Sylvester et al. (1978) to differentiate the apophysis from the core facies. The sub-parallel vertical alignment of the megacrysts in the apophysis was interpreted by Sylvester et al. (1978) to indicate magmatic flow.

More recently, St. Blanquat et al. (1994) have used microstructural criteria to subdivide the Papoose Flat pluton into three domains corresponding to magmatic flow, high (> 500°C), and low (< 500°C) temperature solid-state deformation (Fig. 1). The core of the pluton is primarily characterized by magmatic microstructures which formed at temperatures above the 650°C solidus (Manning 1981) and is surrounded by the high and low temperature solid-state flow domains. Representative microstructures from each of the three domains are illustrated in Fig. 2.

Anisotropy of magnetic susceptibility (AMS) data from the Papoose Flat pluton, combined with microstructural examination of the same samples from which AMS analyses were obtained, indicate that the grain shape foliation and stretching lineation (solid-state deformation) within both the aureole and gneissic border facies of the pluton (Law et al. 1992, 1993) is parallel to magmatic foliation and lineation within the interior of the pluton (St. Blanquat et al. 1994). This interpretation is in agreement with model cooling histories for the Papoose Flat pluton which indicate that both the low temperature solid state domain of the pluton and surrounding aureole rocks were deforming plastically while the pluton core was still above the solidus (Nyman et al. 1995).

Morgan et al. (1998) proposed a two-stage model for the cooling history of the Papoose Flat pluton. Based on andalusite porphyroblast-matrix relationships in the aureole rocks, they argued that the pluton was initially intruded as an inclined sill at the level of the Campito Formation. Heat from the sill thermally weakened the surrounding metasediments and initiated contact metamorphism. Forcible injection of more magma translated (mostly vertically) and attenuated the thermally weakened wall rocks producing a laccolith-like structure. Strain associated with the inflation of the sill drove plastic deformation and dynamic recrystallization of quartz at temperatures of 450°C or higher (Law et al. 1992).

Internal contacts within the pluton provide evidence for multiple injections of magma (St. Blanquat et al., personal communication 1998). The heat and strain provided by additional pulses of magma prolonged the deformation and dynamic recrystallization of the pluton. At the present time little direct evidence establishing the time between magma batch emplacement exists. Solid-state deformation ceased when the pluton interior cooled through its solidus approximately 100,000 years after emplacement (Nyman et al. 1995). The solid-state deformational

Figure 2. Photomicrographs of representative microstructures from: a) magmatic domain, b) high temperature solid-state domain, c) low temperature solid-state domain.

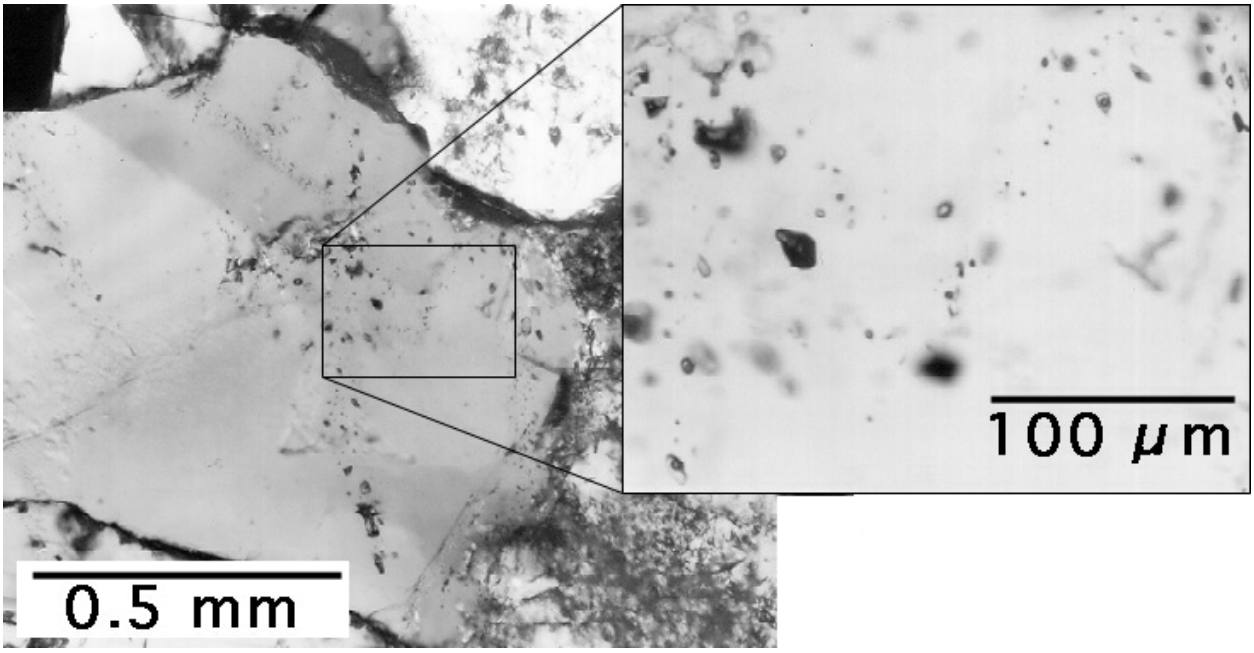

Figure 2a1. Patchy extinction in magmatic domain quartz from granite sample PF39A1. Inset shows two phase aqueous low salinity fluid inclusions typical of deformed quartz grains of the Papoose Flat pluton. Polarized light.

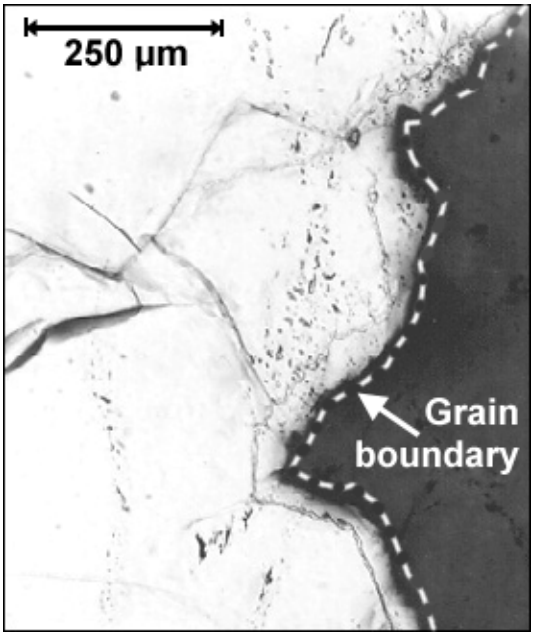

Figure 2a2. Two magmatic domain quartz grains in granodiorite sample PF39A1. The lobate grain boundaries indicate recrystallization by grain boundary migration, which destroyed pre-existing linear arrays of pseudosecondary fluid inclusions. Plane polarized light.

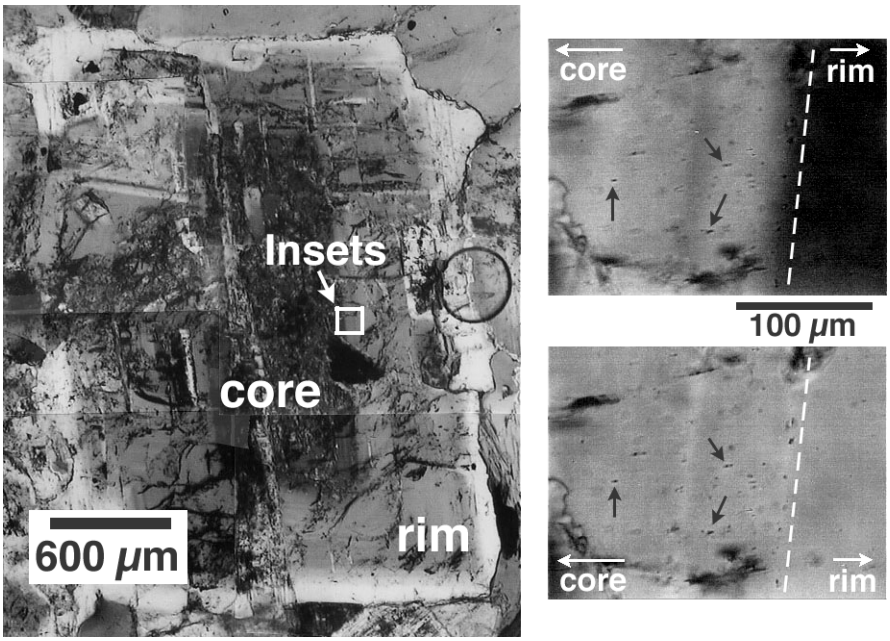

Figure 2a3. The fluid inclusion-rich core of PF 44A1 K-feldspar ends abruptly at the core-rim boundary, indicated by dashed line in the insets. The two insets show the greater abundance of fluid inclusions in the core of the crystal (left of the core-rim boundary) at higher magnification. Black arrows indicate individual fluid inclusions. Left: polarized light. Upper right: polarized light, different extinction angle than left picture. Lower right: plane light.

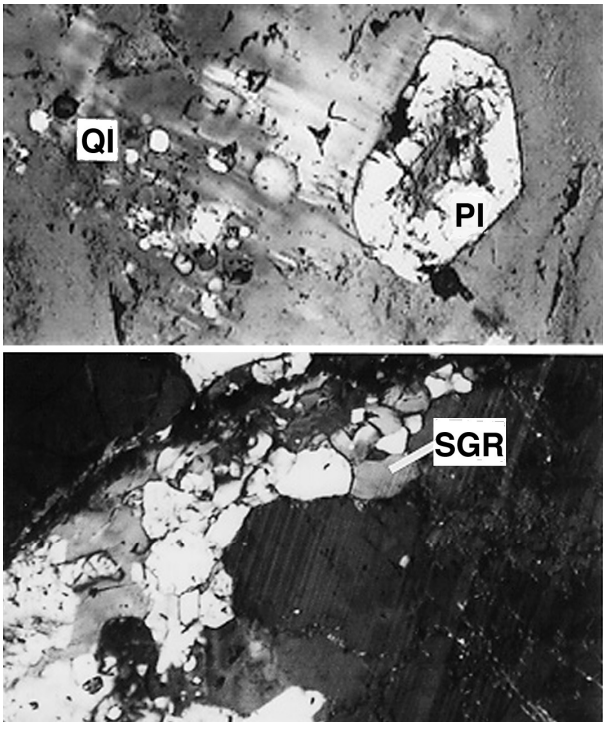

Figure 2b. High temperature solid state deformational microstructures in granite samples PF40 (top) and PF 88 (bottom). Top: Deformation lamellae in large K-feldspar megacryst between quartz and plagioclase inclusions (QI and PI, respectively). Polarized light, 2.5 mm wide. Bottom: Core and mantle structure of feldspar and quartz around plagioclase phenocryst with albite twinning. SGR indicates a grain recrystallized by subgrain rotation. Polarized light, 0.80 mm wide.

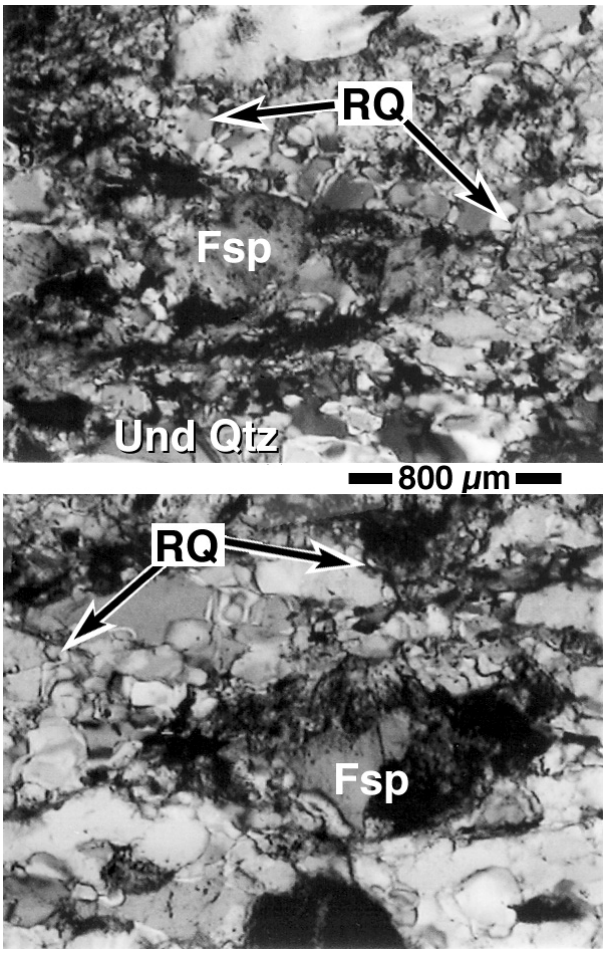

Figure 2c. Low temperature domain microstructures in aplite sample PF91. Ribbon quartz (RQ) defines a gneissic foliation around feldspar augen (Fsp) with undulose extinction in the top and bottom microphotographs. Some of the larger quartz grains in the top photomicrograph display undulose extinction (Und Qtz). Polarized light.

microstructures were interpreted to have been locked in at the end of deformation after the last injection of magma.

MINERALOGY

The Papoose Flat pluton is a hypidiomorphic granodiorite in the west and grades eastward into granite in the apophysis. K-feldspar megacrysts and smaller subhedral quartz porphyroblasts are surrounded by a groundmass of quartz, two feldspars, biotite, and accessory muscovite, magnetite, and ilmenite. Fluorite has been reported from the northern margin of the pluton (Ross 1965). A few weight percent fluorine was also detected in biotite and muscovite by Brigham (1984). The average composition of the K-feldspar megacrysts is $Or_{83}Ab_{15}Cn_2An_0$, where Cn indicates celsian, the barium component (Brigham 1984). The megacrysts contain inclusions of calcic oligioclase (16 vol%), quartz, biotite, muscovite, allanite, magnetite, ilmenite, and apatite (Brigham 1984). Some of the K- feldspar megacrysts and groundmass crystals have converted to microcline with patchy tartan-plaid twinning. The remaining orthoclase megacrysts which have not converted to microcline display oscillatory zonation like that of plagioclase due to variations in Ba content (Brigham 1984). Backscattered electron images of three K-feldspar megacrysts inidcate correlate that the development of patchy tartan-plaid twinning correlates with high Ba zones.

The mineralogy of the Papoose Flat pluton indicates that it was initially H_2O undersaturated (Brigham 1984). Brigham (1984) has reported a few biotite pseudomorphs after hornblende. The absence of hornblende, combined with the mineralogy of the pluton, corresponds to a granodiorite composition with an initial water content of approximately 4 wt% (Naney 1983). The pluton would have reached saturation when the first biotites formed at 85% crystallization

(Brigham 1984). Due to the depth and high total pressure (3.8-4.2 kb) of the pluton, a one phase, high density liquid would have exolved from the magma at saturation (Yang & Bodnar 1994). Quartz+feldspar+biotite±muscovite veins similar to potassic alteration observed in porphyry copper deposits formed late in the cooling history. Pegmatite veins would have formed just before the magma cooled to its solidus of 650°C. The partial alteration of plagioclase and K-feldspar to sericite resemble phyllic alteration seen in porphyry copper deposits. In addition, magnetite was altered to hematite, as well as biotite to chlorite. Some of the K-feldspar reverted to microcline at approximately 475°C (Dickson 1996).

Accurate pressure estimates are essential for the calculation of fluid inclusion trapping temperatures (T_t's). As discussed above, the emplacement pressure of the Papoose Flat pluton is well constrained between 3.8 and 4.2 kb by the intersection of the Mus + Qtz dehydration reaction and the granite solidus (Kerrick 1972) and the aluminosilicate triple point of Bohlen et al. (1991) at 4.2 ± 0.3 kb.

Several geothermometers restrict deformation temperatures to between 420°C and 650°C, the appropriate solidus for a pluton of this composition (Manning 1981). Calcite-dolomite thermometry of carbonate aureole rocks by Nyman et al. (1995) indicated temperature ranges of 380-540°C across the aureole and 420-550°C at the pluton-wallrock contact. Microstructures and quartz c-axis fabrics from plastically deformed quartz veins in the gneissic border facies of the pluton indicate minimum deformation temperatures of 450°C (Law et al. 1992).

ANALYTICAL METHODS

Methodology

Hand samples for fluid inclusion and petrographic analysis were collected along a traverse extending north from the southern margin of the pluton (Fig. 1). Sixteen thin sections were examined to determine the characteristic microstructures of each deformational domain (Table 1).

Microthermometry

Fluid inclusions were examined in eleven doubly polished thick (~ 0.1 mm) sections of granite, quartz+feldpar±muscovite and pegmatite veins, and a single plastically deformed quartz vein (Table 1). For each fluid inclusion assemblage (FIA, Goldstein and Reynolds 1994) within each sample, inclusion composition and homogenization temperatures (T_h's) were determined. Due to the small size (~10 μm diameter) and sporadic occurrence of the granite-hosted inclusions (samples 40, 88, 66C), the larger, more abundant inclusions in later-formed vein samples were also measured. Because no differences were observed between fluid inclusions in granite and

Table 1. Sample descriptions. Samples in italics were only used for microstructural analysis; all other samples wereused for both microstructural and microthermometric analyses. The microstructures of the samples do not neccessarily correlate with the microstructural domain listed above. See Fig. 1 for sample locations.

Number	Description	Location relative to Microstructural Domains
19A2	granite	Magmatic
39A1	granite	Magmatic
40	*granite*	*Magmatic*
44A1	*granite*	*Magmatic*
96A	*Qtz vein*	*Magmatic*
89B	granite	High Temperature
88	*granite*	*High Temperature*
92X	Ksp megacryst	High Temperature
89C	pegmatite vein	High Temperature
92A	Qtz-Fsp-Mus vein	High Temperature
89A	unoriented vein float	High Temperature
87A	*Qtz-Fsp-Mus vein*	*High Temperature*
66C	granite	Low Temperature
66AA	granite adjacent to vein	Low Temperature
66AB1	Qtz-Fsp vein	Low Temperature
91C	Qtz vein - plastically defm.	Low Temperature

vein samples, they must have formed at or reequilibrated at the same PT conditions. The unexpected observation of high temperature solid state microstructures in magmatic domain samples prompted the analysis of inclusions in two additional thick sections of magmatic-domain samples (19A2, 39A1) from the center of the pluton (see Fig. 1 for locations). Fluid inclusion assemblages within each thick section were correlated with microstructures of the host grains. The fluid inclusion data are summarized in the appendix.

Inclusion compositions and homogenization temperatures (T_h's) were determined with a Linkam THMS 600 heating/cooling stage and Leitz OrthoPlan microscope. Temperature profiles were entered into a Linkam TMS 92 computer, which controlled the rate of temperature change during heating and cooling of inclusions. Typical heating and cooling rates ranged from 10 to 60°C/min between temperatures of -120° and +400°C. Trapping temperatures (T_t's) were calculated from the measured T_h's with the FORTRAN programs REVISED ISOCHORE CALC (Bodnar, unpublished data) and NEWTWO V. 2 (Connoly & Bodnar 1983). A few T_t's were calculated from experimentally determined isochores for the 6% NaCl - 10% CO_2 - 90% H_2O system from Schmidt (1997).

Fluid inclusion compositions were determined from eutectic, ice melting, and clathrate melting temperatures. Eutectic temperatures of approximately -21.1°C for aqueous inclusions indicate that NaCl is the dominant salt in the inclusions. The salinities of aqueous inclusions

were calculated from observed ice-melting temperatures with an equation relating freezing point depression of H_2O-NaCl solutions to salinity (Bodnar 1993). The -56.6°C eutectic temperatures of the H_2O-CO_2 inclusions indicates that no other gases are present in the inclusions. H_2O-CO_2 inclusion salinities were similarly calculated from clathrate melting temperatures with the equation of Darling (1991).

DEFORMATIONAL MICROSTRUCTURES

MAGMATIC DOMAIN

Microstructures characterizing the magmatic domain of the Papoose Flat pluton are interpreted to have formed above the solidus temperature of 650°C while the pluton consisted of more than 30% melt (Hibbard 1987). Feldspar phenocrysts and surrounding globular quartz grains characterize magmatic conditions (Hibbard 1987). The majority of the subeuhedral plagioclase phenocrysts are compositionally zoned. A magmatic flow foliation is defined by the alignment of K-feldspar megacrysts and mica laths. The sector zonation of plagioclase inclusions in the K-feldspar megacrysts has been used as evidence for crystallization under magmatic conditions (Brigham 1984). If 30% melt existed during magmatic domain conditions (Hibbard 1987) the melt would have been H_2O undersaturated because H_2O saturation would not be reached until 85% crystallization (Naney 1983, Brigham 1984). Thus primary fluid inclusions could not have been trapped during magmatic flow stage of deformation. This is consistent with the observation that both orthoclase and microcline-hosted fluid inclusions from magmatic domain samples indicate subsolidus trapping temperatures.

In the samples collected, the dominant magmatic microstructures have been overprinted by weakly-developed high temperature solid-state microstructures. Quartz grains exhibit patchy extinction and prismatic subgrains (Fig. 2a1). Lobate quartz grains recrystallized through grain boundary migration (Regime III recrystallization of Hirth and Tullis 1992) producing new generations of quartz grains (Fig. 2a2). In addition, at least two generations of plagioclase and K-spar are present. Altered, fluid inclusion-rich cores are surrounded by inclusion-poor feldspar rims (Fig. 2a3). Some of the inclusion-poor feldspar grains resulted from subgrain rotation. Similar feldspar microstructures are observed in samples collected from all three of the microstructural domains of the pluton.

The overprinting solid-state microstructures in the magmatic domain must have been associated with very small magnitude strains as the dominant microstructures characterizing the magmatic domain are still preserved. Both thermal modeling (Nyman et al. 1995) and AMS analysis (St. Blanquat et al. 1994) indicate that magmatic flow in the center of the pluton was

synchronous with solid-state flow at the pluton margins, with deformation being driven by forceful magma emplacement (Morgan et al. 1998). As the pluton cooled inwards, early magmatic microstructures would have been progressively overprinted by solid-state microstructures.

HIGH TEMPERATURE SOLID-STATE DOMAIN

The dominant microstructures within the high temperature solid-state domain formed between 650 °C (when less than 30% melt would be predicted to remain in the cooling crystal mush - Bouchez et al. 1992) and approximately 500°C. Within this domain, quartz is generally present as elliptical grain aggregates, with individual grains displaying a chessboard pattern of sub-boundaries, a few basal sub-boundaries (c-slip) and perfectly polygonized prismatic sub-boundaries which are frequently dentate due to grain-boundary migration (St. Blanquat et al. 1994). At these temperatures quartz recrystallizes by grain boundary migration and feldspar by subgrain rotation (Tullis and Yund 1987, Gapais 1989, Hirth and Tullis 1992, FitzGerald & Stunitz 1993). Microstructures in both minerals include deformation lamellae and undulose extinction.

Representative high-temperature microstructures of the pluton are illustrated in Figure 2b. K-feldspar megacrysts display perthite lamellae and microcline twinning. Some of the megacrysts have reverted to microcline with tartan plaid twinning. Sericite alteration, recrystallized new grains, and quartz beads occur along the cleavage planes of both microcline and K-feldspar. Deformation twins and lamellae in plagioclase are oriented parallel to foliation defined by aligned mica laths and elongate quartz aggregates. A few of the plagioclase cores display undulose extinction. Subgrain rotation recrystallization has occurred at the edges of some plagioclase crystals. Lobate grain boundaries and lack of internal deformation provide evidence for extensive grain boundary migration recrystallization of the quartz. Most quartz grains display slight undulatory extinction. In addition, biotite in areas of extensive feldspar and quartz recrystallization has been altered to chlorite.

LOW TEMPERATURE SOLID-STATE DOMAIN

With the exception of brittle fracturing of feldspar, the low temperature solid-state microstructures (Fig. 2c) are predominantly of crystal plastic origin. A gneissic foliation located around the margin of the pluton is defined by ribbon quartz and mica laths which anastomose around K-feldspar and plagioclase augen; this domain corresponds to the gneissic border facies recognized by Sylvester et al. (1978). Small recrystallized feldspar grains mantle some of the feldspar augen. Some of the augen, and many of the elongate quartz grains, display undulose extinction. Grain boundary migration (Regime III of Hirth and Tullis 1992) is indicated by lobate

boundaries between adjacent quartz grains. The pattern of crystallographic fabrics in plastically deformed quartz veins from the low temperature solid-state domain indicates minimum deformation temperatures of 450°C (Law et al. 1992, 1993). Overall, microstructures of the low temperature domain are similar to those of the high temperature domain, but with less evidence for quartz grain boundary migration, more elongate quartz grains with undulatory extinction, and the appearance of brittlely fractured feldspars.

FLUID INCLUSION MICROTHERMOMETRY

PETROGRAPHY

The majority of fluid inclusions in the Papoose Flat pluton are two phase, low salinity (<10 wt% NaCl equivalent), liquid rich aqueous inclusions without trapped phases. The inclusions have been grouped into 43 fluid inclusion assemblages (FIA's) based on their room temperature phase relations and temporal classification (primary, pseudosecondary, or secondary[1]). The T_h ranges of the 43 FIA's vary from 0 to 30°C. The number of inclusions within each FIA ranged from two to 11 with a median of four. Fluid inclusion assemblages in K-feldspar, plagioclase, and quartz were analyzed. Four FIA's contain an unidentified, cubic, high relief, and high retardation color crystal. Pseudosecondary and secondary aqueous inclusions from the healing of intra- and intergranular fractures, respectively, displayed the same characteristics. Less common three phase (CO_{2v}, CO_{2l}, H_2O_l) low salinity, liquid-rich inclusions containing 10-20 volume % CO_2 were observed. The CO_2 in most H_2O-CO_2 inclusions homogenized to a liquid or by critical behavior. One of the four FIA's with the unidentified solid phase also contains CO_2. The abundant immature, ragged aqueous inclusions from late fracturing were not studied. Figure 3 illustrates representative inclusions of each type.

The sizes, shapes, and salinities of the inclusions vary widely (Appendix). Quartz-hosted inclusions range from 4 to 80 µm, with a median size of 15 µm. The majority of inclusions in quartz are oval to irregularly shaped. Fluid inclusions in feldspar commonly display a negative crystal shape. Few irregularly shaped inclusions were observed. The sizes of the feldspar-hosted inclusions also span a large range, from 5 to 50 µm, with a median size of 12 µm. Only three inclusions, two in low temperature domain quartz-feldspar vein 66A and one in low temperature granite 66, contained a halite crystal, indicating salinities > 26 wt% NaCl equivalent. The rest of the inclusions had a median salinity of 3.1 wt%.

---

[1]Primary fluid inclusions are trapped along growth zones as a mineral crystallizes. Pseudosecondary fluid inclusions are trapped during mineral growth along fractures which later heal. Secondary fluid inclusions are also trapped along fractures, but after crystallization is complete (Roedder 1984).

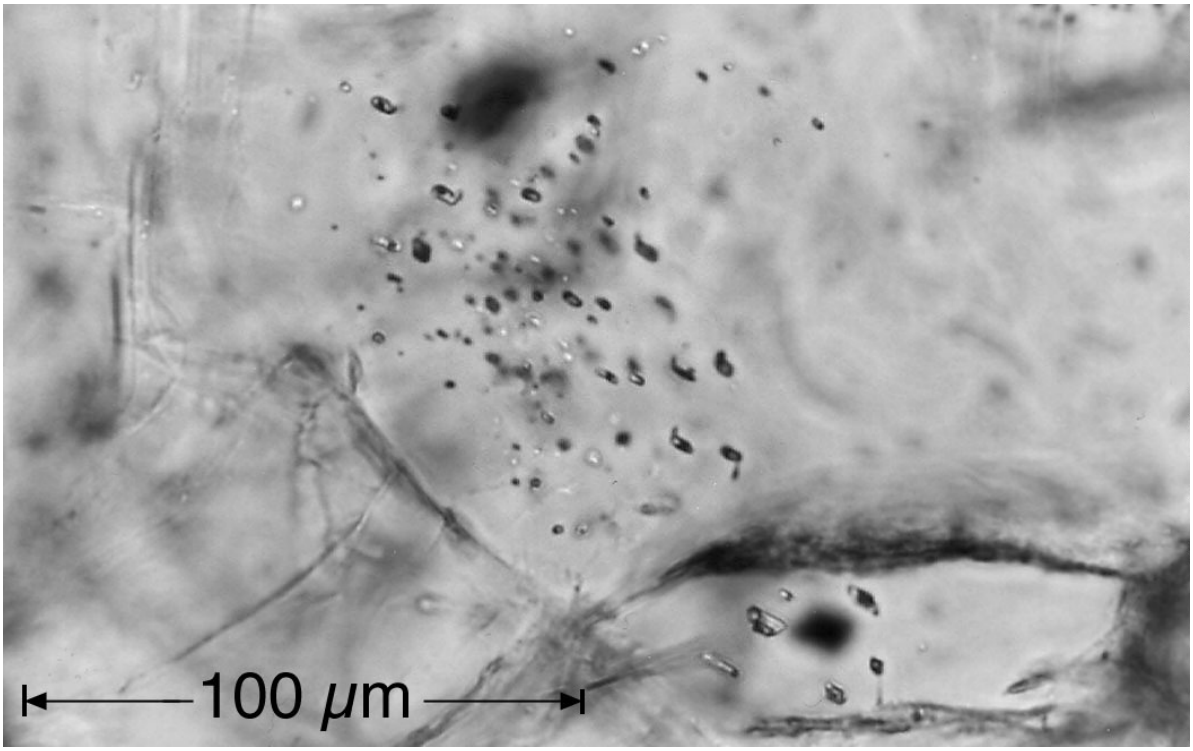

Figure 3a. Aqueous fluid inclusions in orthoclase from high temperature domain sample 89B1,B1.1. Plane light.

Only those fluid inclusions which could clearly be related to deformation were selected for study. The majority of inclusions are hosted by deformed or altered grains. Based on the T_h data presented below, we believe that the original primary inclusions in quartz have been destroyed by recrystallization and recovery. All of the quartz has undergone some degree of crystal-plastic deformation and displays undulose extinction, patchy extinction, or lobate grain boundaries indicative of grain boundary migration recrystallization. Several fluid inclusion-microstructural associations further support this interpretation. Inclusions in quartz are frequently found near lobate grain boundaries (Fig. 2a2, 4a) or triple junctions of recrystallized quartz grains. Linear pseudosecondary arrays of inclusions commonly begin in the middle of a quartz grain and end at a lobate grain boundary at the margin of the grain (Fig. 4b). Areas with deformation lamellae are inclusion-free (Fig. 4c).

In contrast to the ubiquitous evidence for grain boundary migration within quartz grains, no microstructural evidence for grain boundary migration recrystallization was found in any of the adjacent feldspar grains. This presumably indicates that deformation temperatures were not high enough for grain boundary migration recrystallization in the feldspars. A few examples of subgrain rotation recrystallization were found in feldspar grains, but not in any of the studied feldspar grains hosting fluid inclusions. Feldspars contain fluid inclusions trapped during

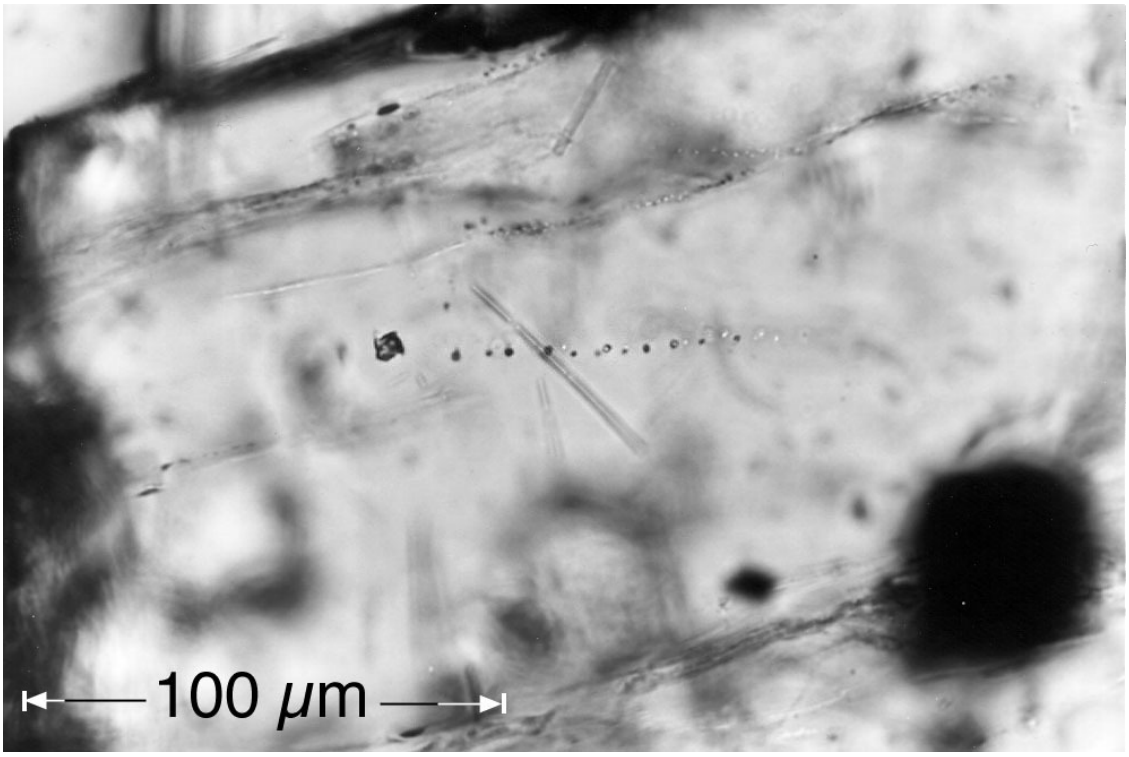

Figure 3b. Pseudosecondary aqueous fluid inclusion in orthoclase from high temperature domain sample 89B1,B1.1. Plane light.

alteration as well as secondary inclusions along fractures. The preserved fluid inclusions with calculated T_t's above 450°C are primary with respect to alteration. Inclusions that are primary with respect to alteration have T_t's above 450°C. Pseudosecondary and secondary inclusions along fractures have T_t's below the feldspar brittle-ductile transition.

MICROTHERMOMETRY

The microstructures of each host grain were noted before measuring the size, shape, composition, salinity, and homogenization temperature (T_h) of each fluid inclusion assemblage. The measured T_h's (and the T_t's calculated from them) overlap significantly between the different host grains and microstructural domains (see Fig. 5a). Overall, FIA median T_h's fell into high and low temperature groups of roughly 145 to 200°C and 200 to 300°C for both H_2O-CO_2 and aqueous FIA's. The lower T_h group is dominated by aqueous FIA's. H_2O-CO_2 FIA's comprise most of the higher temperature group.

Because no direct correlation between the homogenization temperatures of different composition inclusions exists, the corresponding T_t's must be considered. For a given T_h the trapping temperature increases as trapping pressure increases. On average, the T_t's of aqueous

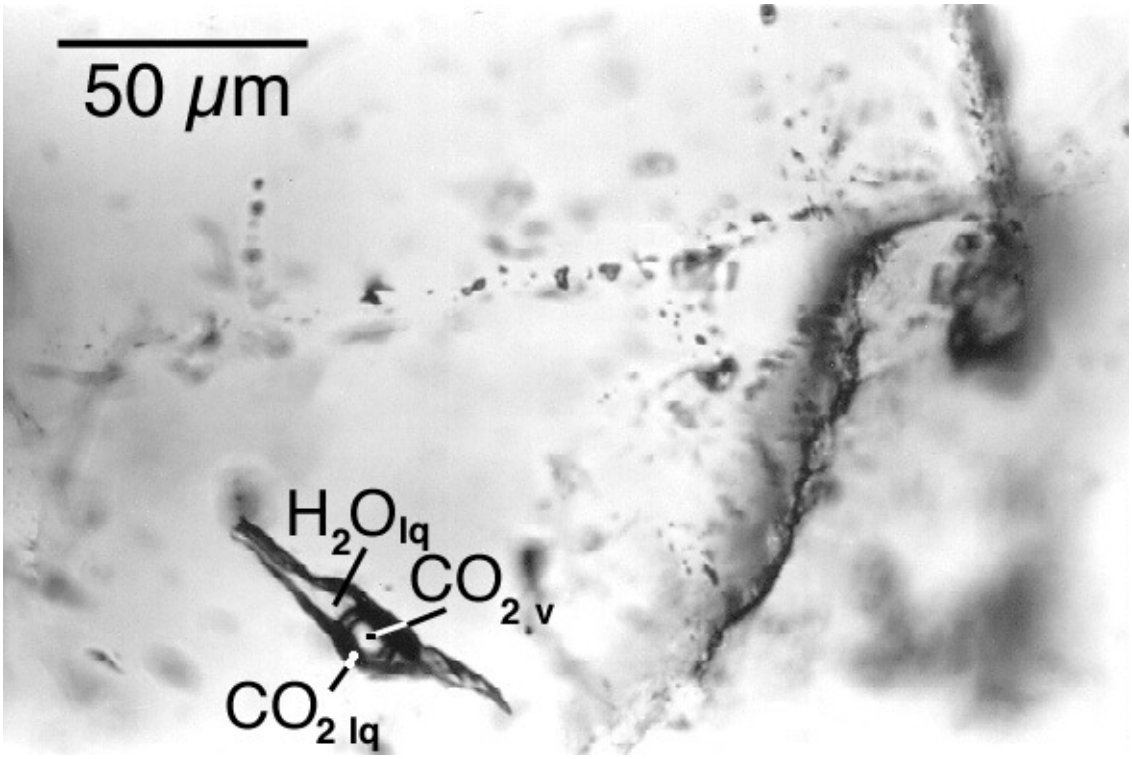

Figure 3c. Large H_2O-CO_2 inclusion in low temperature domain recrystallized quartz grains in granite sample PF66AB3. Liquid water surrounds an outer ring of liquid CO_2 surrounding aCO_2 vapor bubble floats. Plane polarized light.

FIA's increases about 60.8°C with each additional kb of trapping pressure. The T_t's of the average H_2O-CO_2 FIA changes 83.0°C/kb. Most of the T_t's at 4.2 kb for H_2O-CO_2 FIA's range from 400 to 500°C. Only two H_2O-CO_2 FIA's fall in the high temperature group at 554°C and 730°C (Fig. 5b, 6). The aqueous FIA T_t's from both feldspars and quartz range from 360 to 580°C. The corresponding T_t's from FIA's in both minerals are between 360 and 540°C. Although H_2O-CO_2 inclusions in feldspars were observed, only aqueous feldspar-hosted FIA's met the 30°C T_h range restriction for this study.

The T_t's of the myrmekite-hosted FIA and FIA's with the unidentified solid phase span similar temperature ranges. The single FIA in myrmekite has a T_t of 440°C. The T_t's from the H_2O-CO_2 and aqueous FIA's with the unidentified solid phase vary from 419 to 554°C. The inclusions are hosted by four different minerals (quartz, plagioclase, orthoclase, and microcline, respectively) from different microstructural domains and sample types (high temperature domain pegmatite

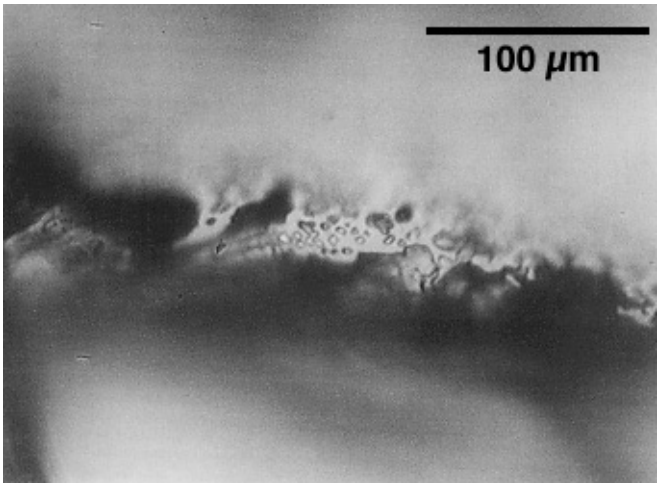

Figure 4a. Fluid inclusions trapped along grain boundaries in high temperature vein sample 89A. Plane polarized light.

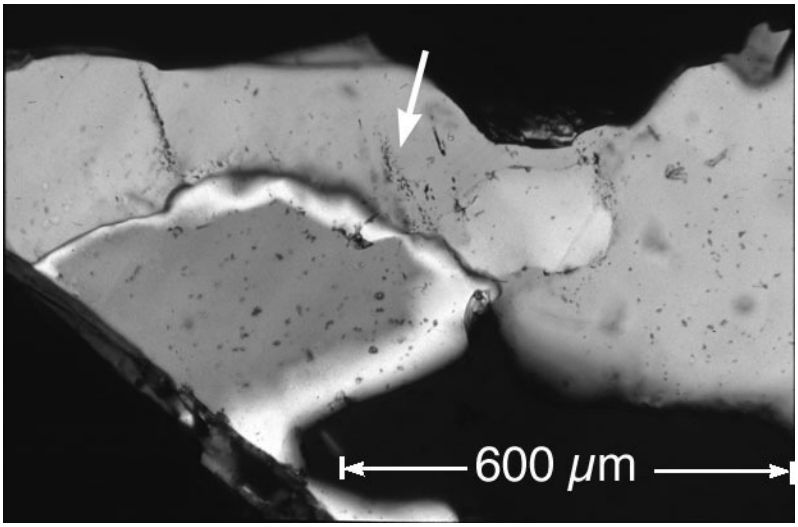

Figure 4b. Grain boundary migration recrystallized quartz from high temperature domain sample 89B1,B1.1. Arrow indicates an area of pseudosecondary aqueous fluid inclusion assemblages. Some of the assemblages are truncated against lobate boundaries between quartz grains. The assemblages are thought to mark the positions of healed microcracks which have been partially overprinted by migrating grain boundaries, and indicate that discrete microcracking events occurred during plastic deformation. Plane light.

veins and magmatic domain granite). The variation in composition, host type, and T_t's suggest that the high retardation color crystals are not daughter minerals, but trapped phases that crystallized earlier than the inclusions themselves.

Only two FIA T_t's are above the granite solidus temperature of 650°C. One is hosted by quartz in low temperature domain quartz-feldspar vein sample 66A, with a median T_t of 673°C from three inclusions. Quartz in low temperature domain granite sample 66C contains the other FIA from three inclusions with a T_t of 730°C. These two FIA's are the most likely to be truly primary inclusions that were trapped under magmatic conditions. The presence of supersolidus trapping temperatures in this vein, which cuts across the solid-state gneissic foliation in the outer part of the pluton, provides evidence for continued expulsion of fluids from the magmatic core of the pluton after initial formation of the gneissic border facies. This rare fluid inclusion data

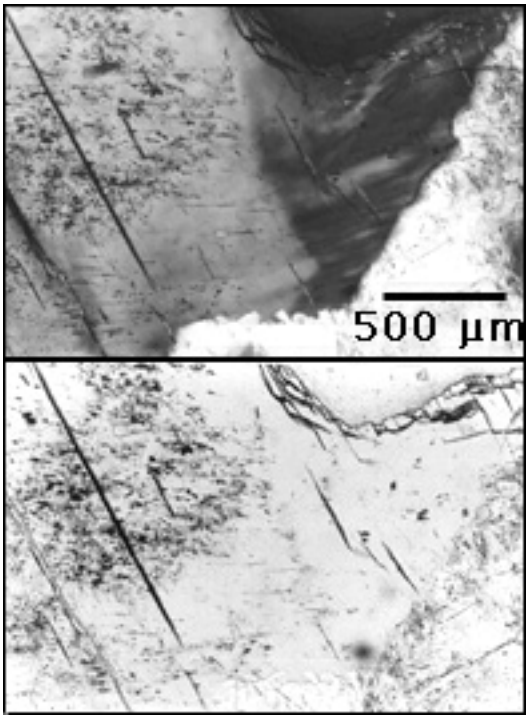

Figure 4c. Deformation lamellae in magmatic domain feldspar (granite sample PF39A1). The undeformed feldspar contains small (<10 µm) fluid inclusions. The areas with deformation lamellae, however, are inclusion-free. The recovery processes that created the deformation lamellae destroyed the primary fluid inclusions. Polarized light.

strongly supports the previous suggestions by St. Blanquat et al. (1994) and Nyman et al. (1995) that plastic flow occurred in both the outer part of the pluton and within its aureole rocks while the core of the pluton was still molten.

The T_t's of the other 41 FIA's record subsolidus temperatures. The subsolidus T_t's indicate that inclusions preserved in all three of the microstructural domains of the pluton were trapped during the last low strain magnitude stages of solid-state deformation. Earlier higher temperature fluid inclusions would have been destroyed by crystal plastic deformation processes. The similar trapping temperatures throughout the pluton are thought to indicate that the preserved fluid inclusions were trapped at progressively later times towards the pluton core, since fluid within inclusions would rapidly equilibrate to a density appropriate for their PT conditions.

DISCUSSION

Three correlations are indicated by histograms of the microthermometric data sorted by host mineral and sample type (Fig. 5a), and by microstructural domain and sample type (Fig. 5b). The histograms and FIA isochore PT diagrams (Fig. 6) illustrate the dominance of subsolidus T_t's consistent with low temperature (< 500°C) microstructural domain trapping conditions across the three microstructural domains. The earlier-formed igneous minerals and the later pegmatite and quartz veins show similar sub-solidus T_t's, so the relative age of the sample does not control

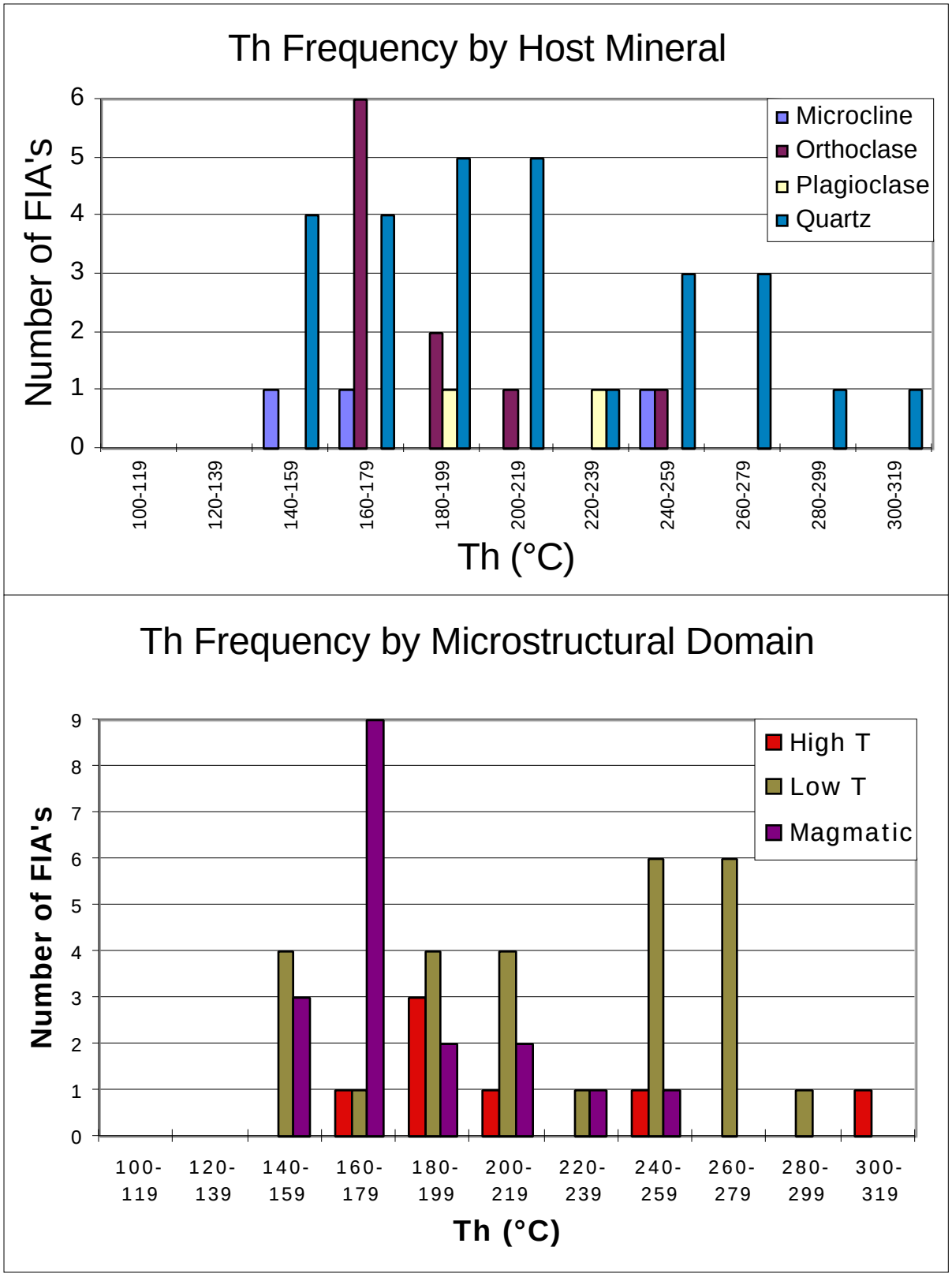

Figure 5a. Histograms showing the frequency of homogenization temperatures (T_h) according to host mineral and within each microstructural domain. Note the overlap of T_h's across the three microstructural domains.

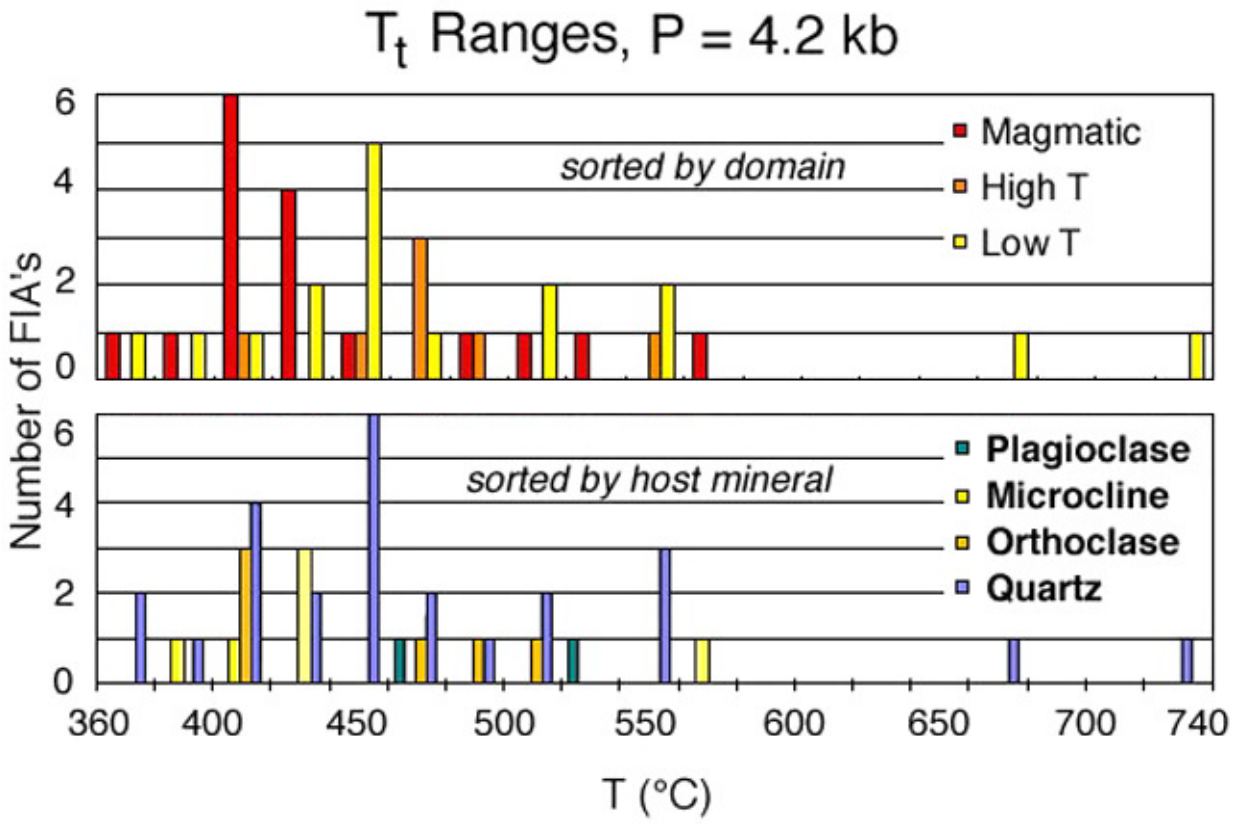

Figure 5b. Histograms showing the frequency of trapping temperatures (T_t) calculated at P = 4.2 kb within each microstructural domain. Note the overlap of T_t's across the three microstructural domains.

trapping temperatures. The number of FIA's clearly increases with decreasing temperature independent of microstructural domain, sample type, and inclusion type, suggesting that no correlation between relative age and trapping temperature exists. As temperatures decreased fewer inclusions were destroyed as brittle deformation became dominant.

The negative correlation between T_t's and number of FIA's suggests that the majority of preserved inclusions reflect late plastic deformation near the transition from ductile to brittle deformation in the deep plutonic environment. There is no correlation between T_t's of the FIA's and the deformational temperatures indicated by the microstructures within each of the microstructural domains of the pluton (Fig. 1). It is likely that the vein- and granite-hosted inclusions were trapped under the same PT conditions, resulting in the overlapping T_h ranges. Only the two supersolidus T_t FIA's[2] could be primary or have trapped the > 600°C fluids (Brigham 1984) that allowed the growth of the K-feldspar megacrysts rims and groundmass. Since the remainder of T_t's are below 550°C, the majority of inclusions may have trapped the

[2] The two supersolidus T_t FIA consist of three aqueous inclusions in quartz in low temperature domain quartz-feldspar vein sample 66A with a median T_t = 673°C and three H_2O-CO_2 inclusions in quartz in low temperature domain granite sample 66C with a median T_t = 730°C.

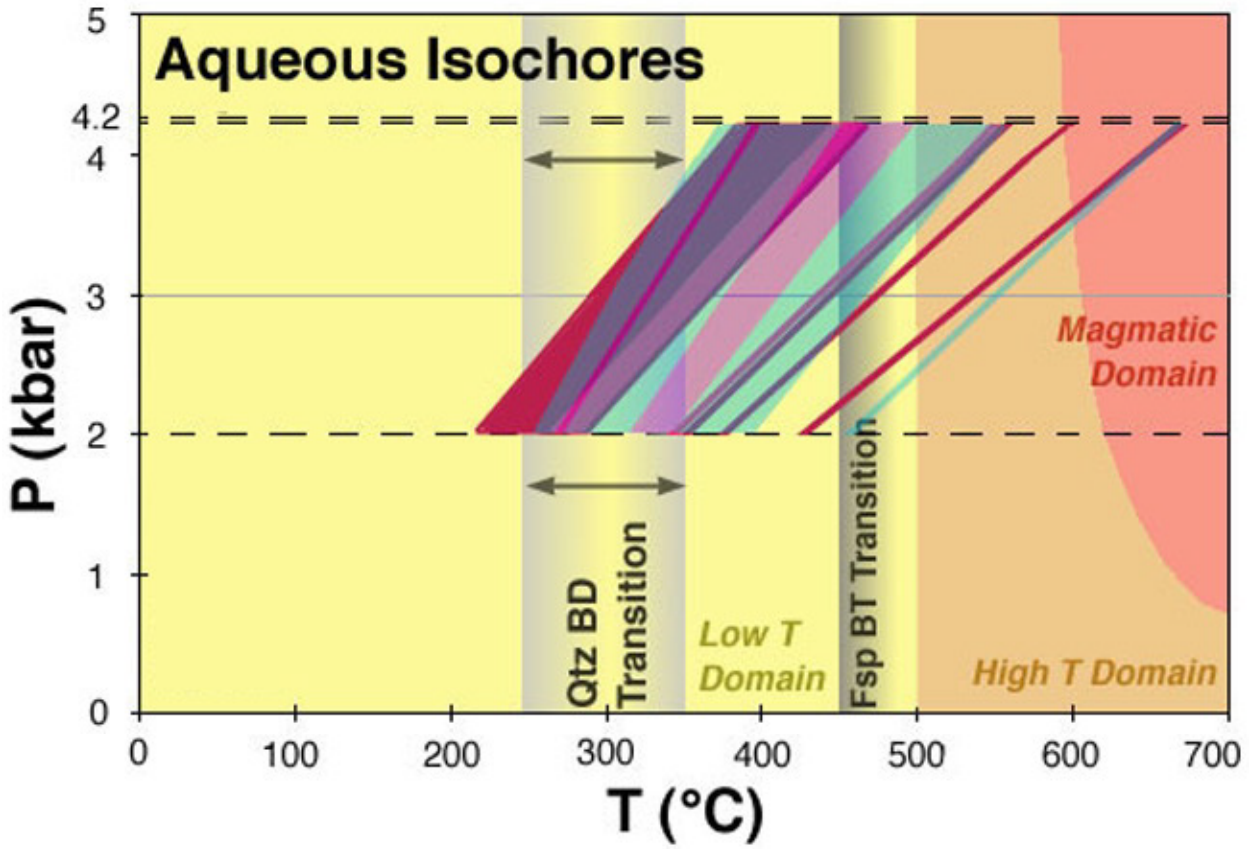

Figure 6a. Isochores showing the pressure-temperature conditions of trapping of the aqueous fluid inclusions of the Papoose Flat pluton. The isochores calculated from the median FIA Th and salinity in the appendix display the possible trapping conditions of inclusions in the three microstructural domains. The red, violet, and blue fields contain the magmatic, high temperature, and low temperature domain isochores, respectively. The isochores illustrate the overlap of T_t's across the three microstructural domains.

fluid responsible for the alteration and disequilibrium isotopic relationships in the pluton. If this is true, following the arguments of Brigham (1984), the trapped fluid originated from magmatic fluids from the eastern end of the pluton.

PRIMARY FLUID INCLUSION ASSEMBLAGES

Except for the two FIA's with supersolidus T_t's, any primary fluid inclusions or inclusions trapped during the formation of the magmatic and high temperature microstructural domains were destroyed or modified by recrystallization and recovery. The homogenization temperatures of isolated, potentially primary inclusions in feldspar were measured. Only two of the calculated trapping temperatures are above the solidus of 650°C, suggesting subsolidus trapping of the majority of inclusions.

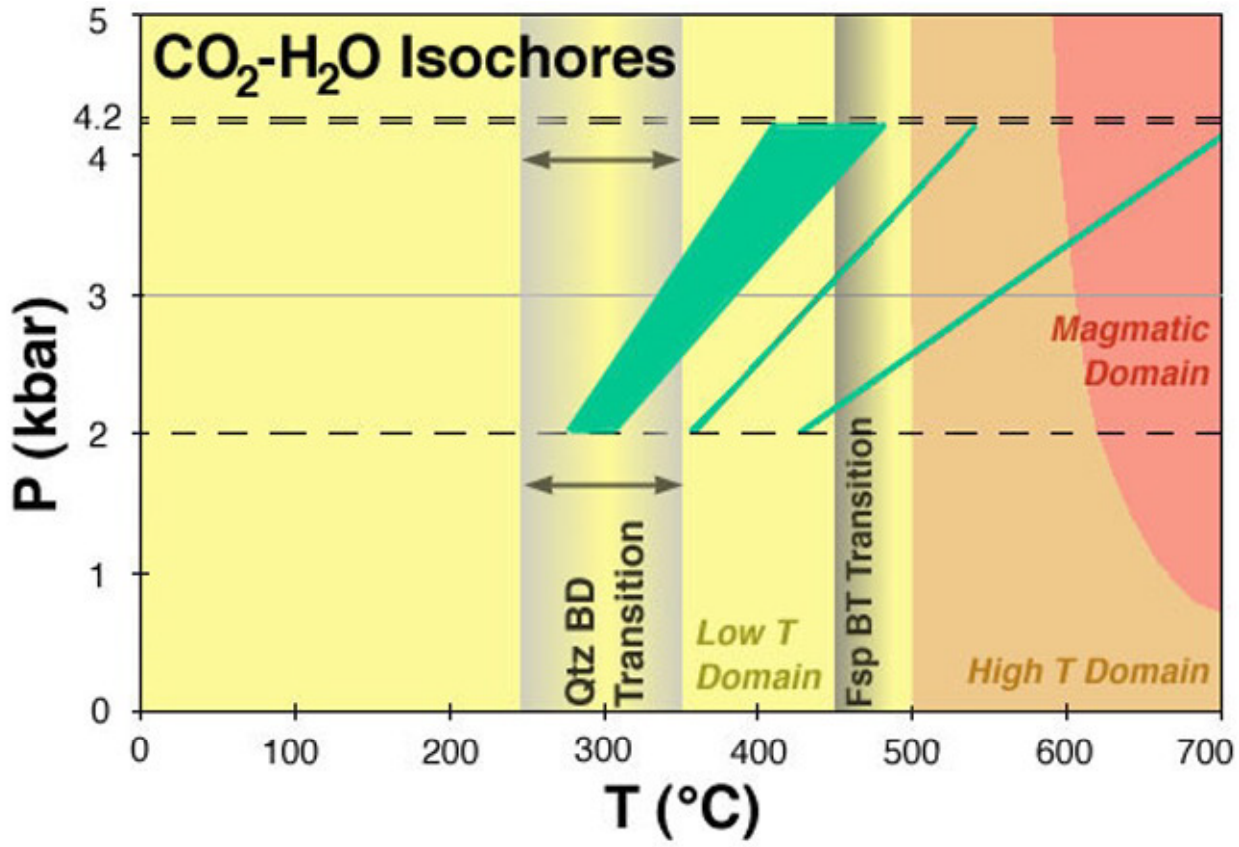

Figure 6b. Isochores showing the pressure-temperature conditions of trapping of the CO_2-H_2O fluid inclusions of the Papoose Flat pluton. The isochores calculated from the median FIA T_h and salinity in the appendix display the possible trapping conditions of inclusions in the three microstructural domains. The aqueous inclusion isochores in Fig. 6a illustrate the overlap of T_t's across the three microstructural domains.

The fact that any primary fluid inclusions were trapped late in the crystallization history (after H_2O saturation at 85% crystallization - Naney 1983, Brigham 1984) suggests metasomatic feldspar growth at subsolidus temperatures. Dickson (1996) proposes that post-crystallization deformation of the pluton provided enough energy to destabilize minerals and drive replacement reactions above 600°C. Dissolution of the surfaces of mineral grains with high resolved compressional stresses would have allowed K-feldspar to grow from intergranular fluids (Dickson 1996). Dickson (1996) cites the occurrence of K-feldspar megacrysts in mafic xenoliths and metasedimentary aureole rocks as evidence for the non-magmatic, metasomatic origin of K-feldspar.

Several facts argue against a completely metasomatic origin of the feldspars. Plagioclase should have begun crystallizing at ~850°C (Naney 1983) and could have trapped inclusions after the magma achieved H_2O saturation. Furthermore, the origin of the K-feldspar megacrysts is controversial. Crystallization of the K-feldspar megacrysts from the magma is supported by the

sector zonation of plagioclase inclusions, absence of granite clasts, and presence of K-feldspar xenoliths and xenocrysts in dikes in the country rock (Brigham 1984).

Both mechanisms probably contributed to the formation of the K-feldspar megacrysts in the Papoose Flat pluton. The high barium megacryst cores crystallized from the magma with oscillatory zonation recording changes in Ba content. The Ba content of the pluton dropped once the groundmass K-feldspar began crystallizing (Brigham 1984). Megacryst rims continued to grow with lower amounts of Ba. Alteration from the circulation of magmatic fluid at T > 600°C altered the preexisting K-feldspar and plagioclase, trapping secondary fluid inclusions along fractures. The onset of subsolidus deformation initiated replacement reactions (Dickson 1996) and the metasomatic growth of new K-feldspar rims. Continued fluid flow below 550°C altered both the metasomatic and magmatic K-feldspar. Sharp discontinuities in inclusion abundance between cores and rims of both feldspars (Fig. 2a3) support alteration of both feldspars, including the metasomatic K-feldspar rims. The formation of myrmekite and the inversion of the high-Ba zones to microcline at ~475°C would have destroyed the earlier formed inclusions. The preserved low T_t inclusions in feldspar hosts represent metasomatic growth of K-feldspar rims and alteration of both feldspars from the circulation of magmatic fluids.

QUARTZ-HOSTED FLUID INCLUSION ASSEMBLAGES

Fluid inclusions in quartz have been observed both as isolated inclusions and in planar arrays within the host grains. The subsolidus T_t's of quartz-hosted FIA's indicate fluid inclusion formation during the late stages of plastic deformation and recovery within the cooling pluton. The abundance of lobate grain boundaries (Fig. 2a2) indicates the dominant role of grain boundary migration in recrystallization of the quartz grains. These microstructures correspond to the experimentally produced high temperature - low strain rate Regime III recrystallization microstructures described by Hirth & Tullis (1992). The absence of primary inclusions (with trapping T_t's near the granite solidus) indicates that multiple waves of grain boundary migration recrystallization have destroyed any fluid inclusions formed during the early crystallization of the pluton. Recrystallization may have eliminated primary inclusions in quartz while creating new fluid inclusions. Griggs (1967) found that annealing of deformed synthetic quartz crystals produced aqueous fluid inclusions. The quartz grain boundary triple junctions observed in this study of the Papoose Flat pluton are compatible with both static recrystallization (i.e. annealing) and dynamic recrystallization in which the rate of recovery is greater than the rate of work hardening.

As temperatures neared the lower temperature limit for quartz grain boundary migration recrystallization, fluid films carried by migrating grain boundaries would break up into an array of fluid inclusions as grain boundary migration became progressively slower (Spiers et al. 1984,

Urai et al. 1986). Multiple pulses of magma intruded at depth within the growing pluton (Morgan et al. 1998) would locally raise the temperature of the overlying and surrounding previously crystallized material, plastically deforming these rocks and triggering new cycles of grain boundary migration in the quartz grains. Within the central magmatic flow domain of the pluton this late stage deformation is represented by the weakly developed solid-state microstructures (e.g. subgrain formation) in the quartz grains. After the final injection of magma, the latest fluid inclusions would be trapped and preserved in the cooling quartz grains. Grain boundary migration ceased when the temperature reached the quartz brittle-ductile transition (BDT) temperature range (250-350°C; Tullis & Hirth 1994 and references therein). However, because different parts of the pluton reached the quartz BDT temperatures at different times, grain boundary migration stopped at tifferent times in different parts of the pluton.

The planar fluid inclusion arrays within the quartz grains formed along microfractures which developed at temperatures above the quartz brittle-ductile transition and were subsequently healed. The presence of planar fluid inclusion arrays which appear to be truncated against lobate quartz grain boundaries (Fig. 4b) indicate that pre-existing microfractures have been partially overprinted by migrating grain boundaries. The large T_t ranges for individual pseudosecondary FIA's discussed below also provide evidence for multiple episodes of dilation and healing along single microfractures. Potential mechanisms for microfracturing within quartz grains at temperatures above the commonly cited crystal-plastic transition are discussed in a later section of this paper.

FELDSPAR-HOSTED FLUID INCLUSION ASSEMBLAGES

At the upper pressure limit of 4.2 kb, most of the feldspar-hosted FIA's yield trapping temperatures below the 450-500°C feldspar brittle-ductile transition (Tullis 1983, Tullis & Yund 1987, Gapais 1989, H. Stunitz 1998, personal communication). Temperatures were not high enough to cause the sweeping grain boundary migration recrystallization that is evident in adjacent quartz grains. A few examples of subgrain rotation recrystallization were found, but none contained fluid inclusions. Fluid inclusions with T_t's above 450°C are primary with respect to alteration. Feldspar-hosted FIA's with T_t's below the brittle-ductile transition trapped fluids along pseudosecondary or secondary fractures.

LARGE T_h RANGE FLUID INCLUSION ASSEMBLAGES

The T_t's of fluid inclusions within an FIA should only vary by a few degrees, since by definition the inclusions were trapped nearly simultaneously. Sixteen of the 43 Papoose Flat FIA's, however, have T_t ranges of over 10°C. The large T_t ranges may be explained by two

mechanisms: some of the inclusions in the FIA have reequilibrated or the fluid inclusions were not all trapped at the same time.

Textural observations of the fluid inclusions do not support reequilibration. Reequilibration occurs when fluid inclusions leak or change in volume (through stretching, for example), which alters the inclusion density and T_h. This hypothesis has been discarded after consideration of the PT cooling path of the pluton. Thermal modeling assuming one batch of magma predicts that the pluton cooled rapidly, with temperatures dropping below the solidus in less than 100,000 years (Nyman et al. 1995 - compare with Morgan et al. 1998). Pressure probably did not change significantly over such a short time period, resulting in a shallow, nearly isobaric PT cooling path for the pluton. The cooling path of the pluton has a shallower slope than those of the isochores of the inclusions. At any given temperature the confining pressure is greater than the pressure inside the inclusion (internal underpressure). Vityk et al. (1994) have shown that the smallest inclusions within an internal underpressure population reequilibrate the most readily when subjected to internal underpressure. The reequilibrated inclusions display characteristic textures, such as scalloped walls or fractures radiating from imploded inclusions. No textures indicative of reequilibration at internal underpressure were observed in the Papoose Flat samples despite the small average inclusion size of approximately 15 μm. The absence of reequilibration textures indicates that reequilibration has not altered the inclusions.

The 16 FIA's with large T_h ranges appear petrographically to have formed simultaneously but were most likely trapped at different times. Eight of the sixteen are pseudosecondary fluid inclusion arrays (Table 2). As the pluton underwent solid-state deformation locally high strains along the edges of some minerals could have caused fracturing during dynamic recrystallization (Lloyd & Knipe 1992, H. Stunitz, personal communication 1998). Intergranular fluid would fill the fracture. Fluid would have been trapped at different times as the fractures slowly healed. This mechanism not only fits the large observed T_h ranges but the common occurrence of pseudosecondary inclusion arrays truncated by a lobate grain boundary (Fig. 2a2, 4b). A migrating grain boundary could sweep across one end of a pseudosecondary inclusion array destroying its internal termination. Figure 4b illustrates such pseudosecondary arrays. This mechanism, however, contradicts the results of experimental studies that show that fractures heal almost instantaneously (Brantley et al. 1990).

Table 2: Pseudosecondary FIA's

FIA	**T_h range (°C)**	**host mineral**
39A1,C1#1	25	plagioclase, core slightly altered
91C,A1#7, 8, 10, 13	17.3, 28, 10, 17.4	vein quartz
89B1,B1.1#3	22.9	quartz
89C,A2#3	14.5	patchy extinction GBM quartz
66A,B1#2	18.7	quartz, H_2O-CO_2 inclusion

The remaining two large T_h range FIA's appear petrographically to have formed simultaneously, but still have a large range (Table 3). Included are isolated inclusions or those along a growth zone in K-feldspar and plagioclase, which were originally thought to be primary. Evidence for a healed pseudosecondary or secondary fracture is difficult to determine petrographically due to the degree of alteration of the feldspar.

Table 3: Other large Th range FIA's

FIA	T_h range (°C)	host mineral
19A2,F1#1	23.1	near rim of microcline with some internal structure, no twinning near inclusions, core altered
89C, A1#4	22.9	along GBM grain boundary in quartz, H_2O-CO_2 inclusion

The composition of the inclusions may also have influenced the FIA's T_h range. The CO_2-H_2O inclusions of FIA 89C, A1#4 may have been trapped at different times in its host quartz as a migrating grain boundary was slowed by relatively high concentrations of CO_2. Mixed CO_2-H_2O inclusions along quartz grain boundaries and triple junctions like those of Papoose Flat samples were observed by Johnson and Hollister (1995) in amphibolite-facies quartz veins in Sardinian schists. Johnson and Hollister (1995) believe that the inclusions were trapped along arrested grain boundaries during grain boundary migration recrystallization of quartz. Preferential trapping of CO_2-rich fluids at migrating grain boundaries could have created the mixed CO_2-H_2O inclusions. The limited solubility of CO_2 in quartz (Walther & Orville 1983) inhibits grain boundary migration around CO_2-rich fluid inclusions. As a result, CO_2-rich fluids are trapped at grain boundaries while aqueous fluids pass through the recrystallizing quartz. The mixed CO_2-H_2O inclusions adjacent to lobate grain boundaries and triple junctions mark the earlier positions of migrating grain boundaries.

Alternately, the scarcity of mixed CO_2-H_2O inclusions could be due to the ease with which CO_2 penetrates quartz-rich rocks via fractures. Brenan & Watson (1988) introduced CO_2 to quartzite samples at run conditions of 0.5 - 1.3 GPa and 1050 - 1200°C. Carbon dioxide penetrated the quartzite at a minimum rate of 0.08 mm/s through a macroscopically visible system of fractures (Brenan & Watson 1988). In the Papoose Flat pluton, CO_2 may have escaped from the cooling rock through a similar network of fractures, minimizing the amount of CO_2 trapped in inclusions.

FLUID INCLUSION AND MICROSTRUCTURAL TEMPORAL RELATIONSHIPS

Model cooling curves calculated by Nyman et al. (1995) for the Papoose Flat pluton are shown in Figure 7. The curves A through D indicate the thermal history for different positions within the pluton and its aureole. Curves A and C correspond to the cooling histories of rocks within the

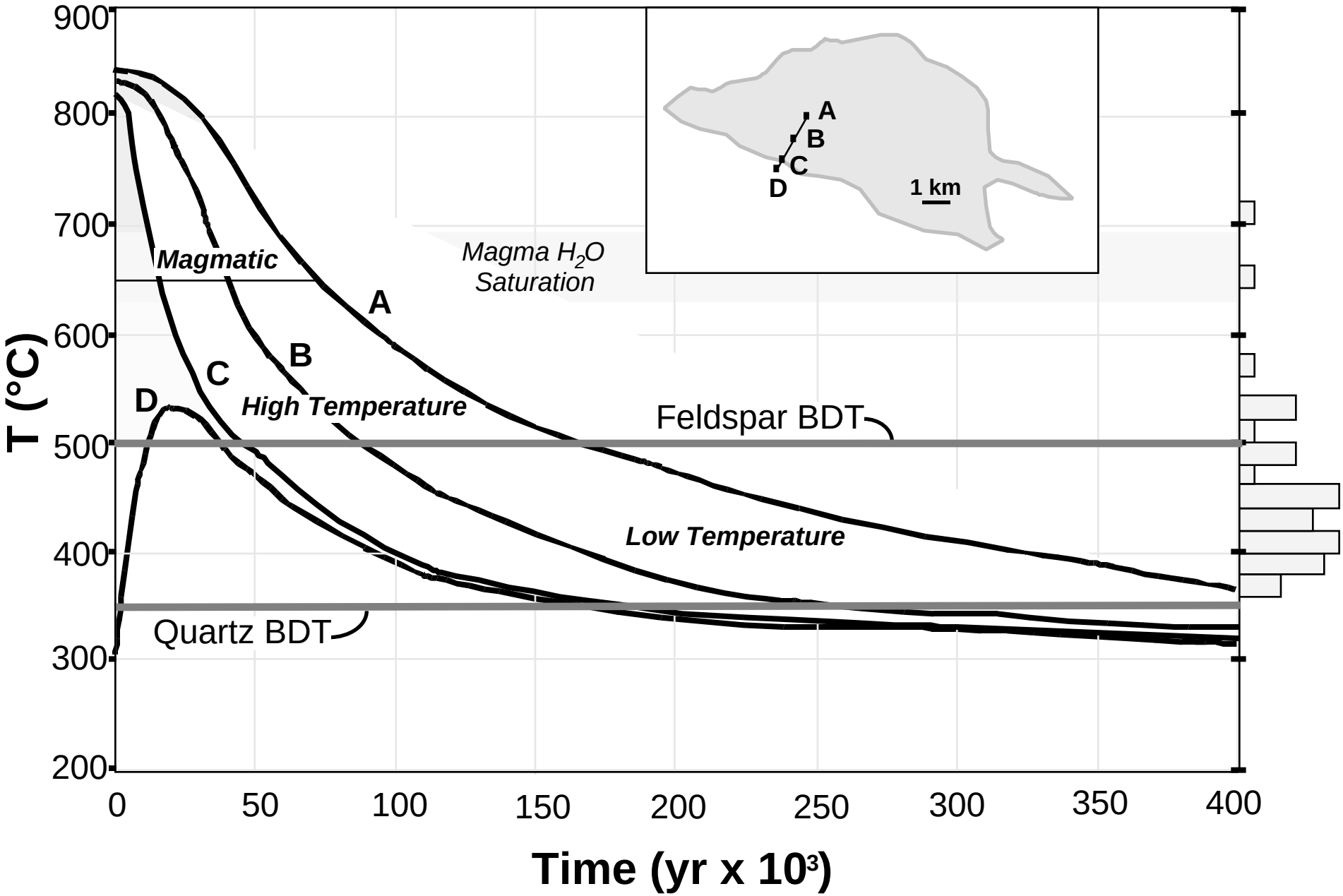

Figure 7. Temporal relationships between formation of microstructures and trapping of fluid inclusions in the Papoose Flat pluton. Complete figure caption follows.

Figure 7. Temporal relationships between formation of microstructures and trapping of fluid inclusions in the Papoose Flat pluton. Curves A through D are cooling paths for rocks at different locations in the pluton, based on the thermal model of Nyman et al. (1995). Curve A corresponds to the cooling paths for rocks at the center of the model pluton; B 6000 m from the model pluton center; C the pluton-wallrock contact; and D 100 m into the aureole from the contact. The model of Nyman et al. (1995) assumes the instantaneous emplacement of one batch of magma at an initial temperature of 850°C and a solidus of 650°C, based on Brigham (1984). The initial wall rock temperature of 250°C is based on a geothermal gradient of 25°C/km at 10 km depth, or 2.7 kb pressure. The intersection of the Mus + Qtz dehydration reaction and the granite solidus (Kerrick 1972) gives a minimum emplacement pressure of 3.8 kb.

Indicated are the temperatures of formation of the magmatic, high temperature solid-state, and low temperature solid-state microstructural domains from St. Blanquat et al. (1994). Also shown are the brittle-ductile transition (BDT) isotherms for quartz (250-350°C; Tullis & Hirth 1994 and references therein) and feldspar (450-500°C; Tullis & Yund 1987, Fitzgerald & Stunitz. 1993). The BDT temperatures of quartz are dependant on strain rate, amount of clay minerals and micas, water content, stress, and grain size (Hirth & Tullis 1994). The chemical composition of feldspar also influences its BDT temperature (H. Stunitz, personal communication 1998).

The relative time at which different portions of the pluton became water saturated is based on studies of synthetic mafic granite and granodiorite melts by Naney (1983). The histogram on the right axis displays the frequency of calculated trapping temperatures (T_t's) for fluid inclusions, assuming a trapping pressure of 4.2 kb (length of the histogram bars have no relation to time on the x axis). The histogram in Fig. 5b shows the same data sorted by microstructural domain. On average, the T_t's of aqueous FIA's change 60.8°C/kb of trapping pressure. The T_t of the average H_2O-CO_2 FIA changes 83.0°C/kb.

magmatic flow and low temperature solid-state deformation regimes of the pluton, respectively. Curve B corresponds to rocks located approximately in the high temperature solid-state regime recognized by St. Blanquat et al. (1994). The model of Nyman et al. (1995) assumes the instantaneous emplacement of one batch of magma (cf. the two phase intrusion model of Morgan et al. 1998) at an initial temperature of 850°C and a solidus of 650°C. An assumed initial wall rock temperature of 250°C is based on a geothermal gradient of 25°C/km at an estimated pluton emplacement depth of 10 km; the corresponding lithostatic pressure was estimated at approximately 2.7 kb (Nyman et al. 1995). However, the presence of primary muscovite in this pluton indicates that total pressure within the pluton may have significantly exceeded this estimated lithostatic pressure. Intersection of the Mus + Qtz dehydration reaction with the granite solidus (Kerrick 1972) gives a minimum total pressure of 3.8 kb. The presence of andalusite in the aureole rocks limits total pressure to a maximum of 4.2 kb (Bohlen et al. 1991).

The simple one dimensional thermal model developed by Nyman et al. (1995) predicts that the Papoose Flat pluton cooled rapidly, approaching pre-intrusion wall rock temperatures of 250°C after 500,000 years. Experimental data from synthetic mafic granite and granodiorite melts (Naney 1983) indicate that the cooling pluton should have become water saturated at between 695°C and 640°C. According to the thermal modeling curves, magma at the pluton-wall rock contact (point C) became water saturated 10,000 to 20,000 years after emplacement. The

interior of the pluton reached water saturation after a longer cooling period. Magma near the center of the pluton (point A) became water saturated 60,000 to 75,000 years after emplacement. The combined water saturation and thermal modeling data for the Papoose Flat pluton indicate that the first fluid inclusions to form in the magmatic domain would have been trapped at a significantly later stage in the pluton's cooling history than the first inclusions to form near the pluton margins.

The majority of inclusions in quartz and feldspar grains from all three of the microstructural domains of the pluton were trapped at temperatures which are higher than commonly cited brittle-ductile transition temperatures for quartz (c. 250-350 °C; e.g. Voll 1976; Sibson 1977, 1984; Scholz 1987) at natural strain rates of 10^{-14} s^{-1}, but lower than the commonly cited transition temperatures for feldspar (c. 450-500°C; e.g. Voll 1976, Tullis 1983) at natural strain rates. At the scale of individual grains, however, these commonly cited transition temperatures should be viewed with caution. For example, Hirth & Tullis (1994) have demonstrated that the transition from fully brittle to fully plastic deformation in quartz aggregates occurs over a wide range of conditions, and that naturally deformed quartzites display microstructural evidence for simultaneous operation of microcracking and crystal plastic deformation mechanisms at temperatures ranging between 200 and 400°C. At the grain scale, feldspars also probably deform by simultaneous microcracking and crystal plastic processes over a wide temperature range. For example, FitzGerald and Stunitz (1993) have documented examples from a range of tectonic settings where albite feldspar recrystallization has occurred at temperatures below 450°C, while in other natural situations microfracturing in feldspar continued up to deformation temperatures of 700-800°C (H. Stunitz, personal communication 1998).

For the Papoose Flat pluton, the lack of correlation between fluid inclusion T_t's and the microstructural domain of host minerals (Fig. 5b) indicates that the observed inclusions were trapped at a relatively late stage in the pluton's cooling history, during the last stages of dynamic recrystallization and recovery, but after development of the microstructural domains. Data from planar fluid inclusion assemblages in some of the quartz grains indicate that microcracking occurred at temperatures above the generally accepted brittle-ductile transition conditions for quartz. This high temperature microfracturing could be due to transient and episodic increases in the local strain rate (cf. Knipe 1989, p. 140), possibly associated with injection of new batches of magma at depth within the pluton (cf. the model of Morgan et al. 1998). Alternatively, microfracturing within the quartz grains may simply have resulted from incompatibilities in deformation behavior and/or thermal contraction between adjacent quartz and feldspar grains (J. Tullis, personal communication 1998) although, at slow strain rates (and slow cooling rates) crystal plastic processes might be expected to inhibit microfracturing (crack blunting - see reviews by Lawn & Wilshaw 1975, Lawn 1983, Atkinson & Meredith 1987, Lloyd & Knipe

1992). Whatever the process, however, microfracturing would have allowed intragranular fluids into the deforming grains, possibly enhancing their deformation.

The results of this study have implications that go far beyond understanding the history of the Papoose Flat pluton. In this study, only a very few fluid inclusion assemblages were found that could have been formed at magmatic conditions (i.e., above the water-saturated solidus), and most inclusions indicate trapping conditions well below the solidus and between the generally accepted brittle-ductile transition temperatures for quartz and feldspar. In contrast, numerous studies of other igneous intrusions have documented the presence of fluid inclusions that were clearly formed in a magmatic environment, at temperatures on or above the water-saturated solidus (Bodnar 1995, Yang & Bodnar 1994, Roedder 1979). The major difference between the Papoose Flat pluton and plutons that do contain magmatic fluid inclusions is that emplacement of the Papoose Flat pluton involved the forceful intrusion of at least two separate pulses of magma (Morgan et al. 1988). As a result, the pluton underwent continuous penetrative deformation during and following crystallization. At the grain scale this protracted deformation history would have resulted in continuous grain boundary migration (at least within the quartz grains) and the destruction of earlier-formed magmatic inclusions. Similarly, plutons emplaced during regional deformation would be expected to have a protracted history of post crystallization deformation. In contrast, plutons which have been passively intruded (e.g. those associated with the porphyry copper deposits in western North America) by mechanisms such as stoping and cauldron subsidence may, particularly in the absence of regional deformation, retain a record of magmatic fluids in fluid inclusions because they have not undergone a complex deformational history during subsequent crystallization and cooling. Thus, the presence or absence of "magmatic" fluid inclusions may be an indicator of the style of pluton emplacement, and the degree of deformation that the pluton experienced during and shortly after emplacement.

CONCLUSIONS

Microstructural analysis of samples collected along a traverse from the margin to the center of the pluton are in agreement with the suggestion by St. Blanquat et al. (1994) that the interior of the Papoose Flat pluton can be divided into three microstructural domains: i) a central core characterized by magmatic microstructures, ii) a middle domain of high temperature (>500°C) solid-state deformation, and iii) an outermost domain characterized by relatively low temperature (<500°C) solid-state deformation. However, weakly developed solid-state microstructures overprint the dominant magmatic microstructures in samples from the core domain. The existence of solid-state microstructures in all three domains indicates that deformation continued during and after crystallization of the interior of the pluton.

Two phase, low salinity (< 26 wt% NaCl equivalent), liquid-rich aqueous fluid inclusions predominate within both quartz and feldspar grains in all samples. Homogenization temperatures overlap for all three microstructural domains. Coexisting andalusite and cordierite in the contact aureole, and the intersection of the Mus + Qtz dehydration reaction with the granite solidus, indicate trapping pressures between 3.8 and 4.2 kb. Of the forty-three FIA's studied, forty one of the trapping temperatures (T_t's) at pressures of 3.8 to 4.2 kb are below the granite solidus of 650°C. Seventy-six percent of the data fall within a temperature range of 350-500°C; i.e. at temperatures which are lower than the commonly cited brittle-ductile transition temperatures for feldspar at natural strain rates, but above those for quartz. No correlation could be established between trapping temperature and either host mineral or microstructural domain within the pluton.

Throughout the pluton, the majority of fluid inclusions are hosted by deformed grains. Feldspar-hosted inclusions are associated with potassic and sericitic alteration or were trapped as secondary or pseudosecondary inclusions along fractures. Inclusions in quartz are frequently found near lobate grain boundaries or near triple junctions; linear pseudosecondary inclusion arrays are commonly truncated against lobate boundaries between adjacent quartz grains. These linear fluid inclusion arrays are thought to mark the positions of healed microcracks which have been partially overprinted by migrating grain boundaries, and indicate that discrete microcracking events occurred during plastic deformation.

The relatively low T_t's indicate that inclusions preserved in all three of the microstructural domains of the pluton were trapped during the last low strain magnitude stages of local solid-state deformation. Earlier higher temperature fluid inclusions, which would have formed after the cooling magma reached water saturation, have presumably been destroyed by crystal plastic deformation processes. The most commonly observed fluid inclusion trapping temperatures (400-500°C) in all three microstructural domains are similar to the deformation temperatures indicated by microstructures and quartz crystal fabrics in the outer part of the pluton, but are obviously lower than temperatures associated with contemporaneous solid state and magmatic flow in the pluton interior. Since fluids within inclusions would rapidly equilibrate to the temperature of their host minerals, the similar trapping temperatures within the pluton core and margin must indicate that the preserved fluid inclusions were trapped at progressively later times traced inward towards the cooling pluton core. However, it remains unclear why the preserved fluid inclusions within all three of the pluton domains should be dominantly trapped at temperatures between the brittle-ductile transitions for feldspar and quartz.

REFERENCES

Arzi, A.A., 1978, Critical phenomena in the rheology of partially melted rocks. *Tectonophysics* **44**, 173-184.

Atkinson, B.K., & Meredith, P.G., 1987, The theory of subcritical crack growth with applications to minerals and rocks. In: *Fracture Mechanics of Rocks*, B.K. Atkinson (Editor), Academic Press, San Diego, 111- 166.

Bateman, P. C., 1992, Plutonism in the central part of the Sierra Nevada Batholith, California, *U. S. Geological Survey Professional Paper 1483*, 186 pp.

Bateman, P. C., Clark, L. C., Huber, N. K., Moore, J. G., & Rinehart, C. D., 1963, The Sierra Nevada batholith: a synthesis of recent work across the central part. *U.S. Geological Survey Professional Paper 414-D*, 46 pp.

Blumenfeld, P., & Bouchez, J.-L., 1988, Shear criteria in granite and migmatite deformed in the magmatic and solid states. *Journal of Structural Geology*, **10**, 361-372.

Bodnar, R. J., REVISED ISOCHORE CALC, Fortran program.

Bodnar, R. J., 1993, Revised equation and table for determining the freezing point depression of H_2O-NaCl solutions. *Geochimica et Cosmochimica Acta*, **57**, 683-684.

Bodnar, R. J., 1995, Fluid inclusion evidence for a magmatic source for metal in porphyry copper deposits. In: *Copper Porphyry Deposits of the American Cordillera*, Pierce, F. W., & Bolm, J. G. (Editors), Arizona Geological Society Digest, **20**, Tucson, AZ, 608-628.

Bohlen, S. R., Montana, A., & Kerrick, D. M., 1991, Precise determinations of the equilibria kyanite - sillimanite and kyanite - andalusite and a revised triple point for Al_2SiO_5 polymorphs. *American Mineralogist*, **76**, 677-680.

Bouchez, J.-L., Delas, C., Gleizes, G., Nedelec, A., & Cuney, M., 1992, Submagmatic microfractures in granite. *Geology*, **20**, 35-38.

Brantley, S. L., Evans, B., Hickman, S. H., & Crerar, D. A., 1990, Healing of microcracks in quartz; implications for fluid flow. *Geology*, **18**, 136-139.

Brenan, J. M. & Watson, E. B., 1988, Fluids in the lithosphere; 2, Experimental constraints on CO_2 transport in dunite and quartzite at elevated P-T conditions with implications for mantle and crustal decarbonation processes. *Earth and Planetary Science Letters*, **91**, 141-158.

Brigham, R. H., 1984, K-feldspar genesis and stable isotope relations of the Papoose Flat pluton, Inyo Mountains, California. Unpublished PhD Thesis, Stanford University, 194 pp.

Burnham, C. W., 1997, Magmas and hydrothermal fluids. In: *Geochemistry of Hydrothermal Ore Deposits*, H. L. Barnes (Editor), John Wiley & Sons, New York, 63-124.

Connolly, J.A.D., & Bodnar, R.J., 1983, A modified Redlich-Kwong equation of state for H_2O-CO_2 mixtures: Application to fluid inclusion studies [abstr.]. *EOS*, 64 (18), 350.

Darling, R. S., 1991, An extended equation to calculate NaCl contents from final clathrate melting temperatures in H_2O- CO_2-NaCl fluid inclusions: Implications for P-T isochore location. *Geochimica et Cosmochimica Acta*, **55**, 3869-3871.

Dickson, F. W., 1996, Porphyroblasts of barium-zoned K-feldspar and quartz, Papoose Flat, Inyo Mountains, California, genesis and exploration implications, In: *Geology and Ore Deposits of the American Cordillera: Geological Society of Nevada Symposium Proceedings,* Coyner, A. R., & Fahey, P. L., (Editors), *Reno/Sparks, Nevada, April 1995*, 909-924.

Ernst, W. G., 1996, Petrochemical study of regional/contact metamorphism in metaclastic strata of the central White-Inyo Range, eastern California. *Geological Society of America Bulletin*, **108**, 1528-1548 .

FitzGerald, J.D., & Stunitz, H., 1993, Deformation of granitoids at low metamorphic grade. I: Reactions and grain size reduction. *Tectonophysics*, **221**, 269-297.

Gapais, D., 1989, Shear structures within deformed granitoids: mechanical and thermal indicators. *Geology*, **17**, 1144-1147.

Gapais, D., & Barbarin, B., 1986, Quartz fabric transition in a cooling syntectonic granite (Hermitage Massif, France). *Tectonophysics,* **125**, 357-370.

Goldstein, R. H., and Reynolds, T. J., 1994, *Systematics of Fluid Inclusions in Diagenetic Minerals: Society for Sedimentary Geology Short Course 31*, Tulsa, Oklahoma, 199 pp.

Griggs, D. T., 1967, Hydrolytic weakening of quartz and other silicates. *Geophysical Journal of the Royal Astronomical Society,* **14**, 19-31.

Hibbard, M.J., 1987, Deformation of incompletely crystallized magma systems: granite gneisses and their tectonic implications. *Journal of Geology*, **95**, 543-561.

Hirth, G., & Tullis, J., 1992, Dislocation creep regimes in quartz aggregates. *Journal of Structural Geology*, **14**, 145-159.

Hirth, G., & Tullis, J., 1994, The brittle-plastic transition in experimentally deformed quartz aggregates. *Journal of Geophysical Research, B*, **99**, 11731-11748.

Johnson, E. L., & L. S., Hollister, 1995, Syndeformational fluid trapping in quartz: determining the pressure-temperature conditions of deformation from fluid inclusions and the formation of pure CO_2fluid inclusions during grain-boundary migration. *Journal of Metamorphic Geology*, **13**, 239-249.

Kerrick, D. M., 1972, Experimental determination of muscovite + quartz stability with $P_{H2O} < P_{total}$. *American Journal of Science,* **272**, 946-958.

Knipe, R. J., 1989, Deformation mechanisms; recognition from natural tectonites, *Journal of Structural Geology*, **11**, 127-146.

Kruhl, J. H., 1996, Prism- and basal-plane parallel subgrain boundaries in quartz: a microstructural geothermobarometer. *Journal of Metamorphic Geology*, **14**, 581-589.

Law, R. D., Morgan, S. S., Sylvester, A. G., 1990, Evidence for large scale shearing during emplacement of the Papoose Flat pluton, California: a re-examination of the microstructures and crystallographic fabrics. *Geological Society of America Abstracts with Programs*, **22**, A183.

Law, R. D., Morgan, S. S., Casey, M., Sylvester, A. G., & Nyman, M., 1992, The Papoose Flat pluton of eastern California: a re-assessment of its emplacement history in the light of

new microstructural and crystallographic fabric observations. *Transactions Royal Society of Edinburgh: Earth Sciences*, **83**, 361-375.

Law, R.D., Sylvester, A.G., Nelson, C.A., Morgan, S.S., & Nyman, M., 1993, Deformation associated with emplacement of the Papoose Flat pluton, Inyo Mountains, eastern California: Geologic Overview and Fieldguide. In: *Crustal Evolution of the Great Basin and Sierra Nevada: Cordilleran - Rocky Mountain Sections, Geological Society of America Guidebook,* Lahren, M.M., Trexler, J.H., Jr., & Spinosa, C. (Editors), Department of Geological Sciences, University of Nevada, Reno, 231-262.

Lawn, B.R., 1983, Physics of fracture. *Journal of American Ceramic Society*, **66**, 83-91.

Lawn, B.R., & Wilshaw, T.R., 1975, *Fracture of Brittle Solids*, Cambridge University Press, 204 pp.

Le Maitre, R.W., 1989, *A Classification of Igneous Rocks and Glossary of Terms: Recommendations of the International Union of Geological Sciences Subcommission on the Systematics of Igneous Rocks*, .Blackwell Scientific Publishers, 193 pp.

Lloyd, G. E., & Knipe, R. J., 1992, Deformation mechanisms accommodating faulting of quartzite under upper crustal conditions. *Journal of Structural Geology*, **14**, 127-143.

Manning, D. A. C., 1981, The effect of fluorine on liquidus phase relationships in the system Qz-Ab-Or with excess water at 1 kb. *Contributions to Mineralogy and Petrology*, **76**, 206-215.

Miller, J. S., 1996, Pb/U crystallization age of the Papoose Flat pluton, White-Inyo Mountains, California. *Geological Society of America, Portland, Abstracts with Programs*, *Cordilleran Section,* **28**, A-91.

Miller, R. B., & Paterson, S. R., 1994, The transition from magmatic to high-temperature solid-state deformation; implications from the Mount Stuart Batholith, Washington. *Journal of Structural Geology,* **16**, 853-865.

Morgan, S. S., Law, R. D., Nyman, M., 1998, Laccolith-like emplacement model for the Papoose Flat pluton based on porphyroblast-matrix analysis. *Geological Society of America Bulletin*, **110**, 96-110.

Naney, M. T., 1983, Phase equilibria of rock-forming ferromagnesian silicates in granitic systems. *American Journal of Science*, **283**, 993-1033.

Nelson, C. A., Oertel, G., Christie, J. M., & Sylvester, A. G., 1972, Structure and emplacement history of Papoose Flat pluton, Inyo Mountains, California*: Geological Society of America Abstracts with Programs*, **4**, 208-209.

Nyman, M. W., Law, R. D., Morgan, S. S., 1995, Conditions of contact metamorphism, Papoose Flat Pluton, eastern California, USA: implications for cooling and strain histories. *Journal of Metamorphic Geology*, **13**, 627-643.

Paterson, S.R., Vernon, R.H., & Tobisch, O.T., 1989, A review of criteria for the identification of magmatic and tectonic foliations in granitoids. *Journal of Structural Geology*, **11**, 349-363.

Paterson, S.R., & Tobisch, O.T., 1992, Rates of processes in magmatic arcs; implications for the timing and nature of pluton emplacement and wall rock deformation, *Journal of Structural Geology*, **14,** 291-300.

Pfifner, O. A., & Ramsey, J. G., 1982, Constraints on geologic strain rates: arguments from finite strain states of naturally deformed rocks. *Journal of Geophysical Research,* **87**, 311-321.

Price, N. J., 1975, Rates of deformation. *Journal of the Geological Society of London,* **131,** 553-575.

Roedder, E., 1979, Origin and significance of magmatic inclusions. *Bulletin of Mineralogy*, **102**, 487-510.

Roedder, E., 1984, Fluid Inclusions. *Reviews in Mineralogy,* Washington D.C.: Mineralogical Society of America, **12**, 644 pp.

Ross, D. C., 1965, Geology of the Independence Quadrangle, Inyo County, California, *U.S. Geological Survey Bulletin,* **1181-0**, 64 pp.

Saint Blanquat (de), M., Law, R. D., Morgan, S., & Bouchez, J., in prep, Internal structure and emplacement of the Papoose Flat pluton.

Saint Blanquat (de), M., Law, R. D., Bouchez, J., & Morgan, S., 1994, Emplacement of the Papoose Flat pluton, White-Inyo Mountains, California: a re-inspection using anisotropy of magnetic susceptibility and microstructures. *Geological Society of America, Abstracts with Programs, Annual Meeting, Seattle,* A-134.

Schmidt, C. S., 1997, Experimental study of the PVTX properties in part of the ternary system H_2O-NaCl-CO_2. Unpublished PhD Thesis, Virginia Tech, 49 pp.

Scholz, C.H., 1988, The brittle-plastic transition and the depth of seismic faulting. *Geologische Rundschau*, **77**, 319-328.

Sibson, R.H., 1977, Fault rocks and fault mechanisms. *Journal of the Geological Society of London,* **133**, 191-214.

Sibson, R.H., 1984, Roughness at the base of the seismogenic zone. *Journal of Geophysical Research,* **89**, 5791-5799.

Spiers, C. J., Urai, J. L., Lister, G. S., & Zwart, H. J., 1984, Water weakening and dynamic recrystallization in salt, *Geological Society of America, Abstracts with Programs, Annual Meeting, Reno*, **16**, 665.

Streckeisen, A. L., 1976, To each plutonic rock its proper name. *Earth Science Reviews*, **12**, 1-34.

Sylvester, A. G., Oertel, G., Nelson, C. A., & Christie, J. M., 1978, Papoose Flat pluton: a granitic blister in the Inyo Mountains, California. *Geological Society of America Bulletin*, **89**, 1205-1219.

Tullis, J., and Yund, R.A., 1987, Transition from cataclastic flow to dislocation creep of feldspar: mechanisms and microstructures. *Geology*, **15**, 606-609.

Tullis, J., and Yund, R.A., 1992, The brittle-ductile transition in feldspar aggregates: an experimental study. In: *Fault Mechanics and Transport Properties of Rocks*, Evans, B. & Wong, T. F. (Editors), Academic Press, 89-117.

Tullis, J., 1983 Deformation of feldspars. In: *Feldspar Mineralogy*, Ribbe, P.H. (Editor), Mineralogical Society of America short course notes, **2**, Washington DC, 297-323.

Urai, J. L., Means, W. D., & Lister, G. S., 1986, Dynamic recrystallization of minerals, In: *Mineral and Rock Deformation Studies, the Paterson Volume*, Heard, H. C. & Hobbs, B. E., (Editors),*American Geophysical Union, Geophysical Monograph*, **36**, 161-199.

Van der Molen, I., & Paterson, M.S., 1979, Experimental deformation of partially melted granite. *Contributions to Mineralogy and Petrology*, **70**, 299-318.

Vityk, M. O., Bodnar, R. J., & Schmidt, C. S., 1994, Fluid inclusions as tectonothermo-barometers: Relation between pressure-temperature history and reequilibration morphology during crustal thickening. *Geology*, **22**, 731-734.

Voll, G., 1976, Recrystallization of quartz, biotite and feldspars from Ersteld to the Leventina Nappe, Swiss Alps, and its geological significance. *Schweizerische Mineralogische und Petrographische Mitteilungen*., **56**, 641-647.

Walther, J. V., & Orville, P. M., 1983, The extraction-quench technique for determination of the thermodynamic properties of solute complexes; application to quartz solubility in fluid mixtures, *American Mineralogist*, **68**, 731-741.

Yang, K., & Bodnar, R. J., 1994, Magmatic-hydrothermal evolution in the "bottoms" of porphyry copper systems; evidence from silicate melt and aqueous fluid in granitoid intrusions in the Gyeongsang Basin, Korea. *International Geology Review*, **36**, 608-628.

APPENDIX

Maroon text = magmatic domain samples, red text = high temperature solid-state domain samples, black text = low temperature solid-state domain samples

FIA	FIA type	median Th (°C)	median Tt (°C) at P = 4.2 kb	salinity (wt %)	FIA Th range (°C)	n	petrography
PF19A2,F1 #1.1	Microcline	149.8	388.9	0.60	23.1	2	microcline, flincs near rim, some internal structure, no microcline twinning near flincs but in other parts of xl, core altered
PF19A2,F2 #8.1	Microcline - trapped phase	170.2	418.9	1.74	11.2	6	microcline groundmass, area with flincs less altered, core altered
PF39A1,C1 #2.1	Myrmekite	194.4	458.3	0.71	21.2	2	myrmekite
PF19A2,F2 #7.2	Orthoclase - ps2nd	160.0	403.6	0.6	13.1	2	perthitic orthoclase, flincs near unaltered rim, core altered
PF39A1,C1 #8.1	Orthoclase	172.0	421.1	0.00	24.6	3	orthoclase, altered core, flincs in growth zone in clear area towards rim
PF89B1,B1.1 #4.01	Orthoclase - ps2nd	195.0	460.0	1.57	27.8	8	twinned orthoclase, little to no alteration, along fracture, ps2nd
PF92X C#1.1	Orthoclase - altered	175.3	426.2	0.00	18.1	2	heavily altered, in growth zone
PF92X C#7.2	Orthoclase - altered	176.2	427.6	0.00	18.8	2	heavily altered, in growth zone
PF92X C#4.2	Orthoclase - altered	216.2	496.2	0.00	0.0	2	heavily altered, in growth zone
PF66A,B.3 #4.3	Orthoclase	242.8	508.2	5.41	5.3	3	clear groundmass orthoclase, flincs aligned with cleavage
PF19A2,C #1.8.1	Orthoclase - ps2nd	165.1	411.1	0.53	4.7	2	
PF19A2,B1 #3.1	Orthoclase - trapped phase	180.0	434.7	1.74	1.7	3	perthitic orthoclase host, altered core, flincs in less altered part towards rim
PF19A2,C #1.8	Orthoclase	165.1	411.1	0.53	4.7	2	twinned orthoclase, heavily altered core, internal structure and def'n twins, flincs in clear, unaltered part of grain
PF39A1,C1 #1.1	Plagioclase	230.5	525.2	0.18	25.0	7	plagioclase (ab twins), core slightly altered
PF89C,A #1.1	Plagioclase - trapped phase, altered	195.9	461.5	1.40	4.0	6	plagioclase (ab twinning), highly altered, some alteration near flincs
PF66A,B.1 #9.1	Quartz	154.5	378.3	7.17	0.0	2	
PF66A,B.1 #10.1	Quartz	154.5	395.4	0.00	1.4	2	
PF92A 3b#4.1	Quartz	170.4	419.2	1.74	26.1	2	
PF91C,A.1 #13.1	Quartz	191.4	453.2	2.90	17.4	4	ps2nd and 2nd (planes) of flincs
PF91C,A.1 #1.3.1	Quartz	197.1	454.8	6.74	5.0	2	ps2nd and 2nd (planes) of flincs
PF66A, A #3.1	Quartz	221.6	503.4	6.16	17.5	3	all in GBM, slight und extn quartz, most flincs along gb's
PF66 C.2#14.1	Quartz	240.8	547.2		7.8	2	
PF66A,B.1 #4.1	Quartz	246.6	548.7	8.28	10.1	2	

FIA	FIA type	median Th (°C)	median Tt (°C) at P = 4.2 kb	salinity (wt %)	FIA Th range (°C)	n	petrography
PF66A, A #7.1	Quartz	290.0	672.0	3.39	23.4	3	all in GBM, slight und extn quartz, most flincs along gb's
PF89B1,B1.1 #3.01	Quartz	217.8	453.4	3.87	9.8	3	chessboard quartz, undulose extinction in area, near edge
PF39A1,C1 #3.1	Quartz - CO2	145.7	494.3	13.23	4.3	2	
PF66A,B.1 #11.1	Quartz - CO2	200.0	548.6	2.44	25.0	2	
PF89C,A1 #4.01	Quartz - CO2	246.6	595.2	3.59	22.9	8	
PF66A,B.1 #2.1	Quartz - CO2	271.3	619.9	10.72	18.7	3	
PF66A,B.1 #13.1	Quartz - CO2	273.1	621.7	3.96	0.0	2	
PF89B1,B1.1 #2.01	Quartz - CO2, ps2nd	181.5	530.1	8.26	22.9	11	GBM, undulose ext quartz, near 3D extension of GBM neighboring grain
PF89C,A1 #3.01	Quartz - CO2, trapped phase	300.0	648.6	4.33	8.0	6	
PF19A2,C #6.1	Quartz - ps2nd	143.0	378.3	1.40	6.8	2	inclusions in same grain as #3 along ps2nd fracture
PF19A2,C #3.1	Quartz - ps2nd	163.8	408.9	1.74	0.0	4	GBM quartz, ps2nd fractures from 3D extension of GBM neighboring grain
PF89C,A2 #3.01	Quartz - ps2nd	166.9	406.0	5.26	14.5	8	patchy extn, GBM quartz, lots of ps2nd flinc arrays, near grain boundary
PF91C,A.1 #8.1	Quartz - ps2nd	178.3	429.7	3.55	28.0	5	ps2nd and 2nd (planes) of flincs
PF91C,A.1 #10.1	Quartz - ps2nd	189.8	444.6	5.71	10.0	2	ps2nd and 2nd (planes) of flincs
PF91C,A.1 #7.1	Quartz - ps2nd	190.9	443.4	6.74	17.3	4	ps2nd and 2nd (planes) of flincs
PF66A, A #4.1	Quartz - ps2nd	200.2	468.1	3.55	3.0	2	all in GBM, slight und extn quartz, most flincs along gb's
PF92A 3b#5.1	Quartz - ps2nd	218.8	501.2	0.00	10.6	3	
PF91C,A.1 #11.1	Quartz - CO2, ps2nd	213.0	561.6	2.63	7.0	3	ps2nd and 2nd (planes) of flincs
PF66 C.2#9(1)	Quartz - CO2, ps2nd	266.0	614.6	6.21	0.0	3	

VITA

Nancy A. Brauer was born on June 26, 1973 in Denville, NJ. In 1991 she began attending the State University of New York at Binghamton and received a B.S. in Geology in May 1995. During the summers of 1994 and 1995 she worked as a research assistant for Colgate University in Hamilton, NY calculating volume change and modal mineral compositions of Taconic slates from microprobe analyses. She pursued a Master's degree at Virginia Polytechnic Institute and State University from 1995-1997. She currently works as a laboratory specialist at the Virginia Tech Fluids Research Lab and is the web developer for the Department of Geological Sciences web site.

_____

Nancy A. Brauer